

1 **Hourly In Situ Quantitation of Organic Aerosol Marker**
2 **Compounds during CalNex 2010**

3
4 **Final Report**

5
6
7 **Contract No. 09-316**

8
9 **Prepared for the California Air Resources Board**

10
11
12 **Principal Investigator**

13 Professor Allen H. Goldstein
14 Department of Environmental Science, Policy and Management
15 University of California Berkeley
16 137 Mulford Hall
17 University of California
18 Berkeley, CA 94720-3114
19 (510) 643-3788
20 ahg@berkeley.edu

21
22
23 **Subcontract to Co-Investigator**

24 Dr. Susanne V. Hering
25 Aerosol Dynamics Inc.
26 935 Grayson Street, Berkeley, CA 94710
27 ph: 510-649-9360
28 fax: 510-649-9361
29 susanne@aerosol.us

30
31
32 **Contributing Researchers**

33 Yunliang Zhao, PhD Candidate, UC Berkeley
34 Dr. Nathan Kreisberg, Senior Research Scientist, Aerosol Dynamics
35 Robin Weber, Staff Research Associate, UC Berkeley
36 Rachel O'Brien, PhD Candidate, UC Berkeley

37
38
39
40
41
42 December 20, 2012
43
44
45

46
47
48
49
50
51
52
53
54
55
56
57

DISCLAIMER

The statements and conclusions in this Report are those of the contractor and not necessarily those of the California Air Resources Board. The mention of commercial products, their source, or their use in connection with material reported herein is not to be construed as actual or implied endorsement of such products.

58
59
60
61
62
63
64
65
66

ACKNOWLEDGEMENTS

We acknowledge John Karlik, Rick Ramirez, and the entire UC Extension Kern County staff, without whom we could not have successfully completed the California Research at the Nexus of Air Quality and Climate Change Project in the San Joaquin Valley. We also thank our collaborators Lynn Russell, Shang Liu, Jennifer Murphy, Jose-Luis Jimenez, Patrick Hayes, Alexander Laskin, and Julian Laskin.

Glossary of Symbols and Acronyms

67		
68		
69		
70	AIM/IC	Ambient Ion Monitor/Ion Chromatograph
71	ARB	California Air Resources Board
72	CalNex	California at the nexus of air quality and climate change
73	CEC	California Energy Commission
74	CMB	chemical mass balance
75	C_{OA}	average OA concentration
76	C_{part}	particle phase concentration
77	CTD	Collection and Thermal Desorption cell
78	C_{total}	total concentration
79	DOE	Department of Energy
80	EC	elemental carbon
81	EPI	Estimated Programs Interface
82	FID	flame ionization detector
83	f_{part}	fraction in the particle phase
84	GC/MS	gas chromatography/mass spectrometry
85	HR-ToF-AMS	High-Resolution Time-of-Flight Aerosol Mass Spectrometry
86	IVOC	intermediate-volatility organic compound
87	k_{om}	gas/particle partitioning coefficient
88	MW	molecular weight
89	NOAA	National Oceanic and Atmospheric Administration
90	O ₃	Ozone
91	OA	organic aerosol
92	OC	organic carbon
93	O/C	oxygen to carbon ratio
94	OH	hydroxide radical
95	PAH	polycyclic aromatic hydrocarbon
96	PM	particulate matter
97	PM _{1.0}	particulate matter < 1 μm
98	PM _{2.5}	particulate matter < 2.5 μm

99	PMF	positive matrix factorization
100	POA	primary organic aerosol
101	Q-AMS	Quadrupole-Aerosol Mass Spectrometer
102	RH	relative humidity
103	SOA	secondary organic aerosol
104	SoCAB	South Coast Air Basin
105	SJVAB	San Joaquin Valley Air Basin
106	SVOC	semi-volatile organic compound
107	TAG	Thermal desorption Aerosol Gas-chromatography mass spectrometry
108	TMB	Trimethylbenzene
109	USEPA	United States Environmental Protection Agency
110	VOC	volatile organic compound
111		

112 **Proposed Tasks and Work Described in this Report**

113
114
115
116
117
118
119
120
121
122
123
124
125
126
127
128
129
130
131
132
133
134
135
136
137
138
139
140

The tasks identified in the original proposal are outlined below:

Task 1. Field Measurements during CalNex 2010

The sampling inlet for TAG was rebuilt to include both a denuder and a bypass line, allowing measurements of organics in both gas and particle phases by the denuder difference method. TAG was deployed at the Bakersfield ground site for the 6 week CalNex field campaign with four continuous weeks of measurements.

Task 2. Data Reduction-Organic Marker Compound Time Lines

More than 100 compounds were identified and quantified in ambient samples collected during the campaign. Both primary and secondary organic marker compounds were identified. Final data was archived in the CalNex database.

Task 3. Data Analysis- Source Attribution through Factor Analysis/Positive Matrix Factorization

The SOA formation mechanisms were investigated by comparing measured fractions of known SOA tracers in particles with predicted. The contributions of various sources to OA were investigated by performing PMF analysis on particle-phase organic tracer compounds. Six types of OA sources were identified, including local POA, a mixture POA and SOA, and four distinct types of SOA. The contributions to OA from these sources and SOA formation pathways related each SOA factor are discussed in detail in Chapter 4.

Task 4. Final Reports

This report is submitted in fulfillment of Task 4.

141
142
143
144
145
146
147
148
149
150
151
152
153
154
155
156
157
158
159
160
161
162
163
164
165

TABLE OF CONTENTS

Disclaimer.....	i
Acknowledgments.....	ii
Glossary of Symbols and Acronyms.....	iii
Proposed Tasks and Work Described in This Report.....	v
Table of Contents.....	vi
List of Figures.....	ix
Abstract.....	x
1. EXECUTIVE SUMMARY.....	1
2. INTRODUCTION AND BACKGROUND.....	5
2.1 Background.....	5
2.2 Our Measurement Approach: On-line Thermal desorption Aerosol GC (TAG).....	6
2.3 Objectives.....	8
3. INSIGHTS FOR SOA FORMATION MECHANISMS FROM MEASURED GAS/ PARTICLE PARTITIONING OF SPECIFIC ORGANIC TRACER COMPOUNDS.....	11
3.1 Introduction.....	11
3.2 Methods.....	13
3.2.1 Sampling and Analysis.....	13
3.2.2 Particle-phase Fraction Calculations.....	16
3.3 Results and Discussion.....	17
3.3.1 Pinonaldehyde.....	19
3.3.2 Phthalic acid.....	22
3.3.3 6, 10, 14-trimethyl-2-pentadecanone.....	24

166	3.4 Conclusions and Implications.....	24
167	3.5 Tables and Figures.....	27
168	4. MAJOR COMPONENTS OF SUMMER-TIME ORGANIC AEROSOL IN BAKERSFIELD,	
169	CA.....	32
170	4.1 Introduction.....	32
171	4.2 Methods.....	35
172	4.2.1 Sampling and Chemical Analysis.....	35
173	4.2.2 PMF Procedures.....	36
174	4.3 PMF Results.....	39
175	4.3.1 Factor 1: Local POA.....	39
176	4.3.2 Factor 2: A mixture of OA sources.....	40
177	4.3.3 Factor 3: SOA1.....	41
178	4.3.4 Factor 4: SOA2.....	41
179	4.3.5 Factor 5: SOA3.....	42
180	4.3.6 Factor 6: Nighttime SOA (SOA4).....	43
181	4.4 Reconstructed OA.....	43
182	4.5 Source contributions to OA mass.....	44
183	4.6 Formation Pathways of SOA.....	45
184	4.7 Conclusions and Atmospheric Implications.....	48
185	4.8 Tables and Figures.....	50
186	5. SUMMARY AND CONCLUSIONS.....	55
187	5.1 Gas-to-particle partitioning (SOA formation).....	55
188	5.2 Major source contributions to OA.....	56
189	5.3 Implications for control of the OA concentrations.....	57

190	6. LITERATURE CITED.....	59
191	APPENDIX A: Supplemental information for Chapter 4.....	66
192	APPENDIX B: Effect of inclusion gas-phase contributions to particle-phase SVOCs on the PMF	
193	solution.....	67
194	APPENDIX C-E. Associated Published Research Papers.....	70
195	APPENDIX F. Data Set Description.....	73
196		

197
198
199
200
201
202
203
204
205
206
207
208
209
210
211
212
213
214
215
216
217
218
219
220
221
222
223
224

LIST OF FIGURES

Figure 3.1	O/C ratios of organic compounds measured by TAG as a function of subcooled vapor pressure at 25°C.....	27
Figure 3.2	Average measured fractions for oxygenated SVOCs and their corresponding reference compounds shown as markers.....	28
Figure 3.3	The temporal change of the cation-to-anion ratio, carboxylic acid group and the fraction of pinonaldehyde in the particle phase.....	29
Figure 3.4	A) Measured fraction of pinonaldehyde in the particle phase as a function of RH B) The average cation-to-anion ratio of inorganic species (sulfate, nitrate and ammonium) as a function of RH.....	30
Figure 3.5	Fraction of phthalic acid in the particle phase as a function of the concentration of gas-phase ammonia.....	31
Figure 4.1	Organic compounds in each factor profile.....	50
Figure 4.2	Box plot of diurnal profile of the mass concentration of each factor and the average diurnal profile of wind direction and the ration of 1,3,5-TMB to toluene.....	51
Figure 4.3	Wind rose plots for six PMF factors using only concentrations larger than the mean concentration in each factor to emphasize the major contributing source directions.....	52
Figure 4.4	Average diurnal cycle of the mass fraction of OA identified as SOA by AMS PMF and by TAG.....	53
Figure 4.5	Mean diurnal mass fraction contribution of each factor to total OA during six different times of day.....	54

225 **ABSTRACT**

226 This study was conducted in Bakersfield, CA to investigate the sources and chemistry
227 controlling aerosol production in the southern San Joaquin Valley Air Basin (SJVAB), a region
228 that is currently out of compliance with air quality standards. To investigate contributions of
229 various sources to organic aerosol (OA) and the formation pathways of secondary organic
230 aerosol (SOA) and subsequently provide insights into effective control strategies to reduce air
231 pollution, an in-situ Thermal desorption Aerosol Gas chromatography-mass spectrometry (TAG)
232 instrument was deployed to measure organic species in both gas and particle phases during the
233 California at the Nexus of Air Quality and Climate Change (CalNex) campaign from May 31st
234 through June 27th, 2010. More than 100 compounds were quantified, including alkanes,
235 polycyclic aromatic hydrocarbons (PAHs), branched PAHs, acids, furanones, and other
236 oxygenated compounds, which provided a large set of organic species for the investigation of
237 SOA formation through comparison between modeled and measured gas/particle partitioning of
238 known SOA tracers and OA source apportionment through positive matrix factorization (PMF)
239 analysis.

240
241 The gas/particle partitioning of phthalic acid, pinonaldehyde and 6, 10, 14-trimethyl-2-
242 pentadecanone, three known oxidation products of hydrocarbons, is discussed in detail to explore
243 SOA formation mechanisms. Measured fractions in the particle phase (f_{part}) of 6, 10, 14-
244 trimethyl-2-pentadecanone were similar to those expected from gas/particle partitioning theory,
245 suggesting that its partitioning is dominated by absorption processes. However, f_{part} of phthalic
246 acid and pinonaldehyde were substantially higher than predicted. The formation of low-volatility
247 products from reactions of phthalic acid with ammonia is proposed as one possible mechanism to

248 explain the high f_{part} of phthalic acid. The observations of particle-phase pinonaldehyde when
249 inorganic acids were fully neutralized indicate that inorganic acids are not required for the
250 occurrence of reactive uptake of pinonaldehyde on particles. The observed relationships between
251 f_{part} of pinonaldehyde and relative humidity (RH) suggest that the aerosol water content plays a
252 significant role in the formation of particle-phase pinonaldehyde. Our results clearly show it is
253 necessary to include multiple pathways in models to predict SOA and include multiple tracers in
254 source apportionment models to reconstruct SOA mass.

255

256 PMF analysis was performed on particle-phase organic species to identify major sources
257 of OA and examine the importance of identified SOA formation pathways. Six OA source
258 factors were identified, including one representing primary organic aerosol (POA), four distinct
259 types of SOA representing local, regional, and nighttime production, and one representing a
260 complex mixture of additional OA sources that were not further resolvable. The average POA
261 contribution to total OA was 15% throughout the campaign. Motor vehicles are suggested to be
262 a major contributor to this POA factor. The four distinct types of SOA contributed a combined
263 72% of total OA. The complex mixture of additional OA sources contributed the rest of total
264 OA. Both regional and local SOA were significant OA sources, but regional SOA had a larger
265 contribution to total OA than local SOA during the day, especially in the afternoon when the
266 observed OA concentration was highest. The contribution of biogenic VOC oxidation products
267 to OA at night was evident, but its contribution is less constrained. The formation of SOA was
268 through multiple pathways, with the largest fraction of SOA formed through condensation of
269 gas-phase oxidation products onto particles. Effective control measures to reduce OA in
270 Bakersfield should focus on reducing sources of organic precursors during the day, especially

271 regional sources. Controlling the species involved in the formation of SOA, such as ammonia,
272 should also reduce the concentration of SOA. However, it is worth noting that the reduction of
273 ammonia emissions could also lead to more nighttime SOA. Further studies are needed to
274 examine effects of the control of ammonia on reductions in OA concentrations.

275 **1.0 EXECUTIVE SUMMARY**

276 The southern San Joaquin Valley Air Basin (SJVAB) is a region that is currently out of
277 compliance with air quality standards. Understanding OA sources and SOA formation is a
278 critical step toward elucidating its roles in climate change and human health and making
279 effective control strategies for air pollution reductions. Previous studies of source contributions
280 to OA in the Bakersfield area were based on the EC-tracer method and chemical mass balance
281 method (CMB) and focused on OA in winter (Magliano et al., 1999; Strader et al., 1999; Schauer
282 et al., 2000). Neither the EC-tracer method nor CMB was able to provide insights into different
283 SOA types. Past work has demonstrated the ability of PMF analysis to separate multiple SOA
284 types with distinct diurnal patterns in the absence of known source profiles in other areas
285 (Williams et al., 2010a). Despite its utility for source apportionment, PMF analysis is not widely
286 performed on organic compounds in the particle phase because it typically requires a larger
287 number of samples which poses significant challenges when measurements of speciated OA are
288 mainly made by filter sampling with 24-hour collection periods in the field followed by solvent
289 extraction in the laboratory for analysis. A thermal desorption aerosol GC/MS (TAG) introduced
290 by Williams et al. (2006) is the first in-situ instrument capable of measurements of speciated OA
291 with hourly time resolution and capturing the trend of gas/particle partitioning in the atmosphere,
292 capable of capturing unprecedented temporal variability in concentrations of organic species.
293 TAG data have been analyzed by PMF in previous work to resolve nine different types of OA in
294 an urban environment, including various SOA and POA sources (Williams et al., 2010a).

295
296 In this study, a TAG was deployed to measure organic species in both gas and particle
297 phases in Bakersfield, CA during the California at the Nexus of Air Quality and Climate Change

298 (CalNex) campaign from May 31st through June 27th, 2010. Prior to the field deployment, the
299 sampling inlet of the TAG was rebuilt using a denuder-based method to separate gases from
300 particles, which represent an improved method to separate gases from particles relative to the
301 filter-based method in the original TAG. Measurements made with this new sampling method
302 enabled the investigation of gas/particle partitioning of oxygenated compounds. Moreover, the
303 particle-phase organic species included in PMF analysis were measured with minimal gas-phase
304 sampling artifacts because the denuder efficiently removed the gas phase organics.

305
306 To investigate the SOA formation pathways, the gas/particle partitioning of three
307 representative compounds including phthalic acid, pinonaldehyde and 6, 10, 14-trimethyl-2-
308 pentadecanone were examined by comparing the measured fractions of these compounds with
309 those predicted by absorptive gas/particle partitioning theory. Our results indicate that absorption
310 into particles is the dominant pathway for 6, 10, 14-trimethyl-2-pentadecanone to contribute to
311 SOA in the atmosphere. Absorption of gas-phase phthalic acid into particles can also contribute
312 to observed particle-phase concentrations, but the major pathway to form particle-phase phthalic
313 acid is likely through reactions with gas-phase ammonia to form condensable salts. The
314 observations of pinonaldehyde in the particle phase when inorganic acids were neutralized
315 indicate that inorganic acids are not required to for the occurrence of reactive uptake of
316 pinonaldehyde on particles.

317
318 Our observations of gas/particle partitioning of oxygenated compounds provided direct
319 evidence that different pathways of gas-to-particle partitioning of organic compounds are present
320 in the atmosphere and are compound-dependent. The non-absorptive gas-to-particle partitioning

321 can improve SOA yields of oxygenated compounds relative to traditional absorptive gas-to-
322 particle partitioning. Our results clearly show it necessary for inclusion of multiple gas-to-
323 particle partitioning pathways into SOA formation models to better account for the contributions
324 of different precursors and formation pathways and the inclusion of multiple SOA tracers into
325 source apportionment models to reconstruct SOA.

326
327 To investigate the source contributions of a variety of sources to OA, PMF analysis was
328 performed on a subset of organic species. The criteria we used for inclusion of compounds were
329 that the timeline of observations covered the entire period of TAG measurements, the
330 compounds were in the particle phase, and the percentage of above detection limit data points
331 was greater than 50% over the full timeline of observations. As a result, 30 compounds in 244
332 samples were included in the PMF analysis. Six OA source factors were identified, including a
333 POA source, a mixture of OA sources, and four types of SOA. Local vehicles are suggested to
334 significantly contribute to POA. The four types of SOA (1-4) displayed distinct diurnal profiles.
335 Three of the SOA factors (SOA1-3) displayed an enhancement in their contributions to OA at
336 different times during the day. SOA1 and 2 were mainly local while SOA3 was more regional.
337 The SOA4 factor mainly occurred during the night and had contributions from both
338 anthropogenic and biogenic SOA. The four SOA factors together accounted for 72% of total OA.
339 Regional SOA (SOA3, 56%) was the largest contributor to OA during the afternoon and
340 nighttime SOA (SOA4, 39%) was the largest contributor during the night. A clear split between
341 local and regional SOA cannot be made during the day. However, the results indicate that
342 regional SOA had a larger contribution to OA than local SOA during the day. The contribution
343 of oxidation products of biogenic VOCs to nighttime SOA was evident, but their contributions

344 were less constrained. These identified SOA types in the atmosphere were formed through
345 multiple formation pathways. The major pathway of SOA 1 and 3 is indicated to be absorptive
346 gas/particle partitioning. The formation of condensable salts play a major role in the formation of
347 SOA2 and reactive uptake of oxygenated compounds on particles contribute to nighttime SOA
348 (SOA4).

349
350 Since SOA was the dominant component of OA, and included four distinct types of SOA
351 which are formed through different formation pathways and impacted by regional sources, the
352 best control strategy for each type of SOA (SOA1-4) to enable effective reductions in the OA
353 concentration may be different. Reduction of SOA precursor emissions on both local and
354 regional scales is needed to reduce the SOA concentration during the day, but control of regional
355 precursor emissions is likely to be most effective in reducing SOA in the afternoon when the
356 observed concentration is highest. Control of ammonia emissions should reduce the
357 concentration of local SOA (SOA2). However, control of ammonia emissions could also lead to
358 more nighttime SOA. Further studies are needed to examine effects of the reduction of ammonia
359 emissions on the reduction in the total OA. At night, because contributions to OA occur from
360 both biogenic and anthropogenic precursors and the split is poorly constrained, it remains unclear
361 if control of anthropogenic SOA precursors could effectively reduce SOA concentration.

362

363

364 **2.0 INTRODUCTION AND BACKGROUND**

365 **2.1 Background**

366 Many urban and rural California air districts are now out of compliance with state and
367 federal air quality standards for particulate matter. Regulatory efforts to conform to PM_{2.5}
368 standards require improvements in our knowledge of the factors controlling the concentration,
369 size and chemical composition of fine PM. While many advances have been made in measuring
370 and modeling the inorganic ionic species that are found in PM, much less is known about the
371 organic fraction. Yet organic matter is a major constituent of airborne particles, comprising 20-
372 80% of the PM_{2.5} mass in many regions (e.g. Schauer and Cass, 2000; Zhang et al., 2007;
373 Williams et al., 2010).

374

375 The chemical composition of atmospheric organic matter is complex. Many hundreds of
376 organic compounds have been identified through chromatography and mass spectrometry
377 techniques (Rogge et al., 1997a, 1997b, 1998; Schauer et al., 1999b; Nolte et al., 1999; Fine et
378 al., 2001). These include alkanes, substituted phenols, alkanals, sugar derivatives, aromatic
379 polycyclic hydrocarbons (PAH), and mono- and di-carboxylic acids. Some organic compounds
380 are markers for primary emissions, such as combustion sources, while others are secondary
381 products formed from anthropogenic or biogenic precursors. Quantitative knowledge of the
382 composition of fine PM organic matter is key to tracing its sources and understanding its
383 formation and transformation processes.

384

385 In 2010, the ARB, the National Oceanic and Atmospheric Administration (NOAA) and
386 the California Energy Commission (CEC) carried out a joint field study of atmospheric processes

387 over California and the eastern Pacific coastal region (CalNex 2010). DOE also participated
388 with both surface sites and aircraft. The goal of the CalNex 2010 program was to study the
389 important issues at the nexus of the air quality and climate change problems, and to provide
390 scientific information regarding the trade-offs potentially faced by decision makers when
391 addressing these two inter-related issues. During this study an instrumented airplane deployed by
392 NOAA flew over both the SoCAB and the SJVAB to provide in situ gas-phase, aerosol and
393 cloud measurements, emissions testing (O₃ and PM precursors and greenhouse gases), regional
394 and inter-regional transport, and day/night O₃ and PM chemistry. The ground sites focused on
395 intensive study of PM and O₃, their precursors, and indicator species to study the chemical
396 production and loss of O₃ and PM. Linking these data sets can address the differences between
397 air quality control strategies needed in the SoCAB and the SJVAB.

398

399 The objective of this work was to identify the origins of fine PM organic matter within
400 the southern San Joaquin Valley of California, a region that is currently out of compliance with
401 PM air quality standards. This was achieved through automated, time-resolved measurements of
402 organic marker compounds in ambient aerosols, combined with source attribution through
403 positive matrix factorization.

404

405 **2.2 Our Measurement Approach: On-line Thermal desorption Aerosol GC (TAG)**

406 Our group has developed the Thermal Desorption Aerosol GC/MS (TAG), an automated
407 system for the in situ characterization of ambient aerosols through gas chromatography and
408 parallel mass spectrometry (Williams et al, 2006). TAG is designed to provide hourly data at the
409 compound level for semi-volatile organic species. While only a subset of the total organic

410 fraction is identified, those compounds that are measured serve as markers for identifying aerosol
411 source types and elucidating variability in the physical and optical properties associated with
412 particulate organic matter. The analytical approach employed by TAG is very similar to
413 published protocols for filter collection and analysis of speciated organics in fine PM. As such,
414 our effort has the advantage of building on the existing source characterization data base for
415 organic compounds. The major difference from filter-based work is that our instrument provides
416 automated, in situ analysis with high time resolution, and avoids known artifacts associated with
417 filter collection (Williams et al., 2006).

418
419 Thermal desorption GC/MS was first applied to the analysis of ambient aerosols by
420 Greaves et al (1985), who employed this approach for the analysis of particles collected through
421 filtration. They found that thermal desorption allowed direct analysis, without the need for filter
422 extraction, and that very small air volumes were sufficient to identify large numbers of species.
423 More recently thermal desorption has been used successfully for the analysis of time-integrated
424 filter and impactor samples of atmospheric aerosols (Waterman et al., 2000, Neusüss et al., 2000,
425 Falkovich and Rudich, 2001). These investigators showed the equivalence of thermal desorption
426 to the more labor intensive solvent extraction methods for the analysis of polycyclic aromatic
427 compounds found in standard reference materials. The method is semi-continuous, with analysis
428 and collection of the next sample occurring simultaneously allowing for hourly time resolution.
429 A full description of the instrumental details has been published (Williams et al., 2006), as have
430 results from actual field measurements (Williams et al., 2007; Goldstein et al. Final report to
431 ARB 2008; Williams et al., 2010; Worton et al., 2011).

432

433 2.3 Objectives

434 There is a critical need for on-line, time-resolved, quantitative measurement of
435 atmospheric particulate organics at the molecular level. Marker compounds unique to specific
436 source types provide a means of determining the relative contributions of various primary
437 sources. Data at the compound level are also needed for understanding the chemical formation
438 and transformation mechanisms leading to secondary organic aerosol formation. This research
439 will provide a useful new data set of immediate value for air quality attainment strategies in
440 California and the development of the State Implementation Plan, and for understanding the
441 pathways leading to secondary organic aerosols that may be of importance in climate change.

442
443 The overall objective of this project was to deploy the TAG instrument for measurements
444 at the Bakersfield field ground site during the CalNex 2010 campaign for approximately 1.5
445 months, with at least four continuous weeks of measurements, in order to investigate tracers and
446 sources of organic PM. Measurements in Bakersfield allowed us to quantify the speciated
447 organic composition in a region with high particulate loadings influenced by agricultural and
448 urban sources. The measurements were part of the larger CalNex 2010 study planned in
449 coordination with the Air Resources Board and the National Oceanographic and Atmospheric
450 Administration (NOAA). The hourly time resolution data from these field measurements was
451 used to improve our understanding of the sources contributing to ambient fine PM organic
452 composition. We used positive matrix factorization and factor analysis to identify the major
453 source types, and we analyzed the data in the context of the broader CalNex 2010 suite of
454 observations.

455

456 Task 1: Field Measurements at the Bakersfield Ground Site

457 To enable the investigation of SOA formation through measurements of gas/particle
458 partitioning and PMF analysis of particle-phase organic species, the sampling inlet of the TAG
459 was rebuilt before this campaign to have two parallel sampling lines, including a denuder line
460 and a bypass line. This modified TAG was deployed at the Bakersfield CalNex Supersite to
461 measure organic species in both gas and particle phases. The sampling flow was alternated
462 between the denuder line to collect particle-phase organics and the bypass line to collect total
463 organics, the sum of gas- and particle-phase organics. Both gas- and particle-phase organics were
464 collected by an impactor cell. Following sampling, the collected organics were thermally
465 desorbed and injected into a gas chromatograph-mass spectrometer (GC/MS) for analysis.
466 During this campaign, TAG measurements were made in two periods wherein their sampling
467 durations were different. The duration of each sample was 90 minutes from May 31st to June 9th
468 (Sampling period I) and 30 minutes from June 10th to 27th (Sampling period II). Over the 27-
469 days of measurements, 244 samples of speciated OA and gas-phase organic species, respectively,
470 were acquired with over 100 particle-phase organic compounds being identified and quantified.

471

472 Task 2: Data Reduction-Organic Marker Compound Time Lines

473 Many compounds were identified using mass spectral and retention time matches with
474 authentic standards. Other resolved compounds, where authentic standards were not available,
475 have been matched to the compounds found in the Palisade Complete Mass Spectral Database
476 (600 K edition, Palisade Mass Spectral Database, Ithaca, NY). More than 100 compounds were
477 identified and quantified in the ambient samples collected during this campaign, covering a
478 broad vapor pressure range and including many functional groups. Both primary and secondary

479 organic marker compounds were identified and quantified, such as hopanes for motor vehicles,
480 retene for biomass burning, phthalic acid for SOA, etc.

481

482 Task 3: Data Analysis-Source Attribution through Factor Analysis/PMF.

483 The gas/particle partitioning of SOA tracers were investigated to provide insights into the
484 pathways of gas-to-particle partitioning whereby oxygenated compounds contributed to SOA.

485 This investigation has identified the occurrence of different formation pathways and shown that
486 effective control strategies to reduce the SOA concentration should be achievable by controlling
487 precursor emissions leading to its formation pathways.

488

489 PMF analysis was performed on the particle-phase organic species to distinguish the
490 contributions to OA from various sources, including primary and secondary sources in this study.
491 Six types of OA sources were identified, including local vehicles, mixed POA and SOA, and
492 four types of SOA. The contributions to OA from these sources, SOA formation pathways, SOA
493 spatial and temporal dispersion, and SOA precursors are discussed in detail in Chapter 4. The
494 roles of different SOA formation pathways are also examined by inclusion of known SOA
495 tracers with their gas-to-particle partitioning pathways being identified. The most effective
496 control strategy to reduce the OA concentration is proposed according to our investigation of
497 SOA formation pathways and contributions of various sources determined by PMF analysis to
498 OA.

499

500 In the following report we describe in detail how each of these objectives were met, the
501 results obtained, and their implications and significance.

502

503 **3. Insights into SOA formation mechanisms from measured**
504 **gas/particle partitioning of specific organic tracer compounds**
505

506 **3.1. Introduction**

507 Secondary organic aerosol (SOA) accounts for the majority of organic aerosol (OA) on a
508 global scale (Kanakidou et al., 2005; Goldstein and Galbally, 2007) and more than 80% in the
509 afternoon during summer in urban areas (Williams et al., 2010a). Understanding the formation
510 and distribution of SOA is important because SOA plays a significant role in affecting climate
511 change on both global and regional scales (Hoyle et al., 2009; Goldstein et al., 2009). However,
512 predictions of SOA by traditional models based on laboratory measurements of SOA yields from
513 volatile organic compounds and absorptive partitioning theory have been shown to substantially
514 underestimate the ambient SOA loadings in polluted regions (Heald et al. 2005; 2010; Volkamer
515 et al., 2006; Spracklen et al., 2011). The discrepancies between measurements and models could
516 in part be attributed to poor understanding of formation pathways of SOA in the ambient
517 atmosphere.

518

519 Laboratory studies have shown that in addition to absorptive gas/particle partitioning
520 following the formation of low-volatility compounds through gas-phase oxidation (Pankow,
521 1994; Seinfeld and Pankow, 2003), other SOA formation pathways such as reactive uptake of
522 gaseous species (Jang et al., 2002; Kroll et al., 2005) and gas-phase non-oxidative reactions (Na
523 et al., 2007) could be important. However, these pathways remain poorly understood. For
524 example, laboratory studies have shown that reactive uptake of oxygenated organic compounds

525 onto acidic particles can significantly increase SOA yields, but there is no agreement on the
526 extent of enhancement of SOA yields (Jang et al., 2002; Iinuma et al., 2005; Kroll and Seinfeld,
527 2008). Additionally, laboratory studies of reactive uptake of oxygenated compounds have
528 focused primarily on small carbonyl compounds and found that not all of them significantly
529 contribute to SOA when their concentrations used in the laboratory studies are scaled to
530 atmospheric levels (e.g., Jang et al., 2002; Kroll et al., 2005). As a result, the contribution of
531 individual compounds to SOA cannot be generalized based solely on their functional groups.
532 Ambient measurements are important to examine the importance of laboratory proposed SOA
533 mechanisms.

534

535 Ambient measurements with an Aerodyne Quadrupole Aerosol Mass Spectrometer (Q-
536 AMS) have been made to examine the effects of aerosol acidity on SOA formation and the
537 results showed that no significant enhancement in SOA formation was observed during acidic
538 periods identified based on the inorganic ion charge balance (Zhang et al., 2007). However, the
539 importance of acid-catalyzed reactions in SOA formation might not be evident using the
540 inorganic ion charge balance as the indicator of aerosol acidity because organic acids could also
541 provide sufficient acidity for the occurrence of these reactions (Gao et al., 2004). Additionally,
542 the variability in the amount of SOA formed through acid-catalyzed reactions could be obscured
543 by SOA formed through other pathways if there is not an analytical method to distinguish them.
544 Through time-resolved speciated measurements of gas- and particle-phase organic compounds,
545 concentrations of organic compounds involved in acid-catalyzed reactions can be determined and
546 SOA products formed through acid-catalyzed reactions can be distinguished from other
547 pathways. Moreover, these measurements provide information to examine factors affecting SOA

548 formation that have previously been investigated in laboratory studies, such as relative humidity
549 (RH) and acidity, and discover new pathways of SOA formation in the atmosphere (Pankow,
550 1994; Jang et al., 2002; Tillmann et al., 2010).

551
552 Williams et al. (2010b) demonstrated that a Thermal desorption Aerosol Gas
553 chromatography (TAG) instrument was able to capture the trend of gas/particle partitioning of
554 individual species, wherein a filter-based sampling method was used to separate gases from
555 particles. In the current study, a denuder-based sampling method was used, representing an
556 improved method to separate gases from particles (Turpin et al., 2000). The investigation of
557 different SOA formation pathways is made by conducting time-resolved, speciated
558 measurements of gas/particle partitioning of oxygenated semi-volatile/intermediate-volatility
559 organic compounds (S/IVOCs) in the ambient atmosphere with this modified TAG. The factors
560 affecting these pathways are investigated using temporal variability of measured gas/particle
561 partitioning of organic species in combination with supporting measurements, such as RH. This
562 study improves the understanding of SOA formation in the ambient atmosphere and likely lead
563 to useful parameterization of SOA formation.

564

565 **3.2. Methods**

566 **3.2.1. Sampling and Analysis**

567 A modified TAG instrument was deployed to measure organic species in both gas and
568 particle phases during the CalNex campaign from May 31st to June 27th, 2010 at the Bakersfield
569 California Supersite. The modification was made before this field campaign by adding an

570 activate charcoal denuder (30 mm OD, 40 cm length, ~490 channels, Mast carbon, UK) into the
571 sampling inlet as a parallel sampling line to a bypass line made of stainless steel tubing. The
572 denuder was housed inside a home-made aluminum cylindrical tube with a tapered cap in each
573 end connecting to the sampling line upstream and downstream.

574

575 A detailed description of TAG can be found elsewhere (Williams et al., 2006; Worton et
576 al., 2011). Only the sampling and operation relevant to this study are described here. During the
577 sampling, ambient air was sampled at 10 L/min from the center of a main flow, drawn from
578 approximately 5 meters above ground at 200 L/min through a 6-inch (i.d.) rigid duct, and
579 sampled through a sharp cut PM_{2.5} cyclone (10 L/min, BGI Inc., Waltham, MA). Downstream of
580 the cyclone, a flow split was made to discard 10% of air flow. Subsequently, 90% of the ambient
581 flow was sampled through the denuder line (or bypass line) and delivered into a customized
582 Collection and Thermal Desorption cell (CTD) through a 9 L/min critical orifice for collection of
583 organics. The aerodynamic particle diameter corresponding to 50% collection is ~0.07 μm so
584 that the entire accumulation mode mass falls within the instrument's collection range (Williams
585 et al., 2006). Gas/particle separation was achieved by alternating ambient air between the
586 denuder and the bypass line. The samples collected through the denuder ("denuded samples")
587 were expected to be only particle phase organics while those collected through the bypass line
588 ("undenuded samples") were the total organics, the sum of the collected gas and particle phase
589 organics. The sampling duration of each sample was 90 minutes from May 31st to June 9th
590 (Sampling period I) and 30 minutes from June 10th to 27th (Sampling period II). The CTD was
591 maintained at 28°C during the ambient sampling and was continuously held at the same
592 temperature for one minute to purge residual air out of the CTD with a helium flow of 20 ml/min

593 at the conclusion of ambient sampling. Following the purge, the thermal desorption of collected
594 organics was carried out in a helium flow by heating the CTD from 28°C to 300°C at a rate of
595 ~30°C/min and held at 300°C for nine minutes followed by thermal injection into a gas
596 chromatograph. The chromatographic separation of organic species was achieved by a capillary
597 GC column (Rxi-5Sil MS; 30 m length, 0.25 mm i.d., 0.25 µm film thickness, Restek). The GC
598 oven temperature was held at 45°C for 18 minutes for the sample injection from the CTD to GC
599 followed, in order, by: 1) a ramp to 150°C at 15°C/min; 2) a ramp from 150°C to 330°C at
600 9°C/min and 3) a hold at 330°C for 4 minutes. Identification and quantification was achieved
601 using a quadrupole mass spectrometer (Agilent, 5973) calibrated based on responses to authentic
602 standards that were manually injected into the CTD at regular time intervals throughout the
603 campaign (Kreisberg et al., 2009).

604

605 The gas collection efficiency of the denuder was determined in the beginning, middle and
606 end of the campaign using the difference of the amount of gas-phase organics downstream of the
607 denuder and bypass lines with a FiberfilmTM glass fiber filter (Pall Corp.) placed upstream of the
608 cyclone to remove particles. Particle penetration through the denuder was determined using an
609 optical particle spectrometer (model UHSAS, Droplet Measurement Technologies) to measure
610 the number size distributions of ambient particles at the inlet and outlet of the denuder before this
611 campaign.

612

613 A broad suite of complementary measurements were concurrently made at this site,
614 including a full range of meteorological, trace gas and aerosol measurements. The measurements
615 utilized in this study included non-refractory PM_{1.0} inorganic and organic aerosol components,

616 carboxylic acid group, gas-phase ammonia and meteorological data. Non-refractory PM_{1.0}
617 aerosol components were measured using a High-Resolution Time-of-Flight Aerosol Mass
618 Spectrometer (HR-ToF-AMS; Aerodyne, Billerica, MA) using the methods described in Liu et
619 al. (2012). PM_{1.0} was also collected by Teflon filters for measurements of the organic acid group
620 (-COOH) by Fourier Transform Infrared (FTIR) spectroscopy (Liu et al., 2012). Gas-phase
621 ammonia was measured using an Ambient Ion Monitor/Ion Chromatograph (AIM-IC) (Markovic
622 et al., 2012).

623

624 3.2.2. Particle-phase Fraction Calculations

625 Because the particle-phase and total organics were not collected simultaneously,
626 measured fraction of a given compound in the particle phase (f_{part}) in sample n is calculated
627 using the particle-phase concentration ($C_{part,n}$) divided by the average of the previous and
628 subsequent total concentrations ($C_{total,n-1}$, $C_{total,n+1}$):

$$629 \quad f_{part} = \frac{2C_{part,n}}{C_{total,n-1} + C_{total,n+1}} \quad (3.1)$$

630 The gas/particle partitioning coefficient (k_{om}) for absorptive partitioning into organic aerosol is
631 calculated by the equation described by Pankow (1994):

$$632 \quad k_{om} = \frac{RT}{10^6 P_L^0 \delta MW} \quad (3.2)$$

633 where R is ideal gas constant ($8.2 \times 10^{-5} \text{ m}^{-3} \text{ atm mol}^{-1} \text{ K}^{-1}$), T is temperature (K), P_L^0 is the vapor
634 pressure of the pure compound (atm) at the temperature of interest, δ is the activity coefficient of
635 the compound in the absorbing phase, and MW is the average molecular weight (g mol^{-1}) of the

636 absorbing phase. The particle-phase fraction based on partitioning theory ($f_{\text{part},T}$) was calculated
637 from the partitioning coefficient constant (k_{om}) and the mass concentration of organic aerosols in
638 $\mu\text{g m}^{-3}$ (C_{OA}):

$$639 \quad f_{\text{part},T} = \left(1 + \frac{1}{k_{om} \times C_{\text{OA}}} \right)^{-1} \quad (3.3)$$

640 The data collected by other instruments were averaged according to TAG sampling
641 duration of 30 or 90 minutes. The average OA concentration (C_{OA}) from HR-ToF-AMS
642 measurements was $3.7 \pm 1.8 \mu\text{g m}^{-3}$ ($0.5 - 11.2 \mu\text{g m}^{-3}$). Average temperature was $26 \pm 6 \text{ }^\circ\text{C}$ ($12 -$
643 40°C). In our study, the theoretical fractions of organic species in the particle phase were
644 calculated using the average temperature and average OA concentration ($T = 26^\circ\text{C}$, $C_{\text{OA}} = 3.7 \mu\text{g}$
645 m^{-3}) and both molecular weight ($\text{MW} = 200 \text{ g mole}^{-1}$) and activity coefficient ($= 0.3$ and 3) from
646 literature (Pankow, 1994; Seinfeld and Pankow, 2003). Subcooled vapor pressures used in this
647 study were from The Estimation Programs Interface (EPI) Suite developed by the US
648 Environmental Protection Agency's Office of Pollution Prevention and Toxics and Syracuse
649 Research Corporation (SRC).

650

651 **3.3. Results and Discussions**

652 More than 150 compounds were measured by TAG, covering a broad vapor pressure
653 range and different functional groups (Figure 3.1). Most identified compounds were present in
654 the vapor pressure range of S/IVOCs defined by Robinson et al., (2007) (Figure 3.1). The
655 gas/particle partitioning of three oxygenated compounds, pinonaldehyde, phthalic acid and 6, 10,
656 14-trimethyl-2-pentadecanone, is discussed in detail to explore SOA formation in the ambient

657 atmosphere. Pinonaldehyde is a major product of α -pinene ozonolysis with gaseous yields of
658 pinonaldehyde being 0.39-0.69 (Liggio and Li, 2006). Phthalic acid and 6, 10, 14-trimethyl-2-
659 pentadecanone have been used as SOA tracers in chemical mass balance model and positive
660 matrix factorization model calculations (Zheng et al., 2002; Shrivastava et al., 2007; Williams et
661 al., 2010a).

662

663 Average collection efficiencies of the denuder for pinonaldehyde, phthalic acid and 6, 10,
664 14-trimethyl-2-pentadecanone were over 98%. Average losses of the particle number inside the
665 denuder were less than 10% for particle sizes spanning the particle spectrometer's range
666 (0.05~1 μm). Though f_{part} of the compounds of interest were overestimated in this study because
667 their gas-phase organics were only partially collected by the collection cell which was designed
668 for collecting particle-phase organics, the extent of overestimation can be indicated by f_{part} of n -
669 alkanes. The gas/particle partitioning of n -alkanes can be well described by the gas/particle
670 absorptive partitioning theory (Fraser et al., 1997) and n -alkanes have the lower or same
671 adsorption coefficient constants on the surface of sampling substrates, relative to other
672 compounds with the same vapor pressure (Goss and Schwarzenbach, 1998). As a result,
673 measured particle-phase fractions of n -alkanes, the sum of absorptive gas/particle partitioning
674 and overestimation caused by incomplete collection of their vapors, are the upper limit of the
675 overestimation of TAG measurements in the vapor pressure range of these n -alkanes.

676

677 The reference compounds selected based on the similar subcooled vapor pressure for
678 pinonaldehyde, phthalic acid and 6, 10, 14-trimethyl-2-pentadecanone are n -tetradecane, n -
679 heptadecane and n -nonadecane, respectively (Figure 3.2). If measured particle-phase fractions of

680 these oxygenated organic compounds are far larger than those of their reference compounds, as
681 is the case for phthalic acid and pinonaldehyde, additional SOA formation pathways must occur,
682 beyond absorptive gas/particle partitioning and overestimation due to under collection of gas-
683 phase organics.

684

685 **3.3.1. Pinonaldehyde**

686 The mean f_{part} of pinonaldehyde was $20 \pm 20\%$, which was much higher than that of its
687 reference compound, *n*-tetradecane (Figure 3.2). The fraction of pinonaldehyde in particles was
688 observed to increase as RH increased (Figure 3.3A), but the fraction contributed by its
689 partitioning into aerosol water is negligible even if a ratio of aerosol water to the dry aerosol
690 mass equal to one was used and all of the aerosol water is available to take up pinonaldehyde.
691 Moreover, this assumed ratio of the water content to dry mass is inconsistent with the average
692 RH of 34% observed during TAG measurements because a ratio of generally less than 0.3 is
693 expected at this average RH (Khlystov et al., 2005; Schuster et al., 2009; Engelhart et al., 2011).
694 The measurements of particle-phase pinonaldehyde reported here were with negligible sampling
695 artifacts due to adsorption of gas-phase pinonaldehyde to the collection cell because the denuder
696 efficiently removed organic vapors. Therefore, our observations of particle-phase pinonaldehyde
697 clearly show that gas-phase pinonaldehyde had been converted into forms with the lower vapor
698 pressures prior to the collection.

699

700 Low-volatility compounds (e.g. oligomers) formed from monomers with direct
701 involvement of pinonaldehyde have been observed in chamber experiments (Tolocka et al.,

702 2004; Liggo and Li, 2006; Tillman et al., 2010) and ambient samples (Tolocka et al., 2004). In
703 our study, low-volatility compounds were measured as a pinonaldehyde monomer, consistent
704 with previous TAG measurements in a forest area (Worton et al., 2011). The reason may be
705 attributed to the use of the thermal desorption method which could decompose low-volatility
706 compounds into their original monomers (Jang et al., 2002). These low-volatility compounds
707 were not directly measured in our study, but the variability in the measured concentration of
708 pinonaldehyde can still be used to investigate factors affecting the formation of low-volatility
709 compounds. In the following discussion, the term of particle-phase pinonaldehyde is taken to
710 include all low-volatility compounds formed with direct involvement of pinonaldehyde. The
711 cation-to-anion ratio, calculated using molar concentrations of ammonium and anions
712 ($=2 \times [\text{sulfate}] + [\text{nitrate}]$) measured by HR-ToF-AMS, is used as an indicator of availability of
713 acids in our study. The presence of excess ammonium is indicated when the cation-to-anion ratio
714 is greater than one and the presence of excess acids is indicated when the ratio is less than one.

715

716 Particle-phase pinonaldehyde was observed while the cation-to-anion ratio was greater
717 than one, indicating that the presence of inorganic acids were not required for the formation of
718 particle-phase pinonaldehyde (Figure 3.4). The excess ammonium observed in particles is
719 attributed to particle-phase organic acids. Since FTIR measures carboxylic acid as an acid group
720 ($-\text{COOH}$) (Russell et al., 2009), excess organic acids were obviously present in particles (Figure
721 3.4). Our observations demonstrate the results from chamber experiments of α -pinene ozonolysis
722 that oligomers are formed on the neutralized ammonium sulfate particles (Gao et al., 2004;
723 Tolocka et al., 2004) and organic acids produced from gas-phase hydrocarbon oxidation are
724 sufficient to catalyze these heterogeneous reactions (Gao et al., 2004).

725

726 Laboratory studies have shown that high aerosol acidity leads to the high yield of
727 oligomers from pinonaldehyde (Liggio and Li, 2006) and oxidation products of α -pinene (Gao et
728 al., 2004; Tolock et al., 2004). However, the laboratory observed trend was not displayed by the
729 relationship between f_{part} of pinonaldehyde and the organic acid group measured by FTIR
730 (Figure 3.4). The reason could be that the contribution of organic acids to the aerosol acidity
731 cannot be directly indicated by their concentration because different organic acids have different
732 dissociation constants and organic acids and their conjugate base can serve as a buffer solution.
733 The cation-to-anion ratio of inorganic ions showed a general trend that the high cation-to-anion
734 ratio was along with the low f_{part} of pinonaldehyde (Figure 3.4), but the acidity estimated based
735 on the cation-to-anion ratio would have large uncertainties when the cation-to-anion ratio is near
736 one (Xue et al., 2011). Moreover, this trend was not observed when other factors affecting the
737 relationship between aerosol acidity and f_{part} of pinonaldehyde were considered, such as RH
738 (Figure 3.3B) which can change the composition and mass of SOA (Nguyen et al., 2011) and the
739 aerosol acidity (Liggio and Li, 2006). As shown in Figure 3.3A, f_{part} of pinonaldehyde displayed
740 a positive dependence on RH in Sampling Period I, consistent with previous TAG measurements
741 in a forested area (Worton et al., 2011). However, the cation-to-anion ratio calculated from
742 inorganic ions did not consistently decrease as RH increased (Figure 3.3B). As a result, the effect
743 of the aerosol acidity on f_{part} of pinonaldehyde is not shown by the relationship between the
744 cation-to-anion ratio and the f_{part} of pinonaldehyde observed in our study.

745

746 In comparison with Sampling Period I, f_{part} of pinonaldehyde was generally lower in
747 Sampling Period II and showed a different dependence on RH (Figures 3.3A and 3.4) while this

748 pattern was not observed for its reference compound, *n*-tetradecane. The different relationship
749 between f_{part} and RH observed during the two sampling periods is also supported by another
750 independent measurement of the cation-to-anion ratio which was different in two sampling
751 periods (Figures 3.3B and 3.4). Therefore, the observed difference between f_{part} of pinonaldehyde
752 on RH represents the real relationship between them in the atmosphere. The high f_{part} of
753 pinonaldehyde was not observed at the elevated RH in Sampling Period II, although the particle-
754 phase concentration of pinonaldehyde was observed to increase as RH increased. The
755 relationships between RH and f_{part} of pinonaldehyde suggest that RH favors the formation of
756 particle-phase pinonaldehyde in the atmosphere, but it is not the main factor affecting the
757 formation of particle-phase pinonaldehyde. Further studies are needed to examine the effect of
758 RH on the yield of particle-phase pinonaldehyde in the atmosphere and laboratory.

759

760 **3.3.2. Phthalic acid**

761 The mean f_{part} of phthalic acid was $60 \pm 20\%$, substantially higher than that of its
762 reference compound, *n*-nonadecane (Figure 3.2). To reproduce the mean f_{part} for phthalic acid
763 using gas/particle partitioning theory, a substantially lower activity coefficient ($\sim 5 \times 10^{-3}$) than the
764 estimated range from 0.3 to 3 for SOA in the atmosphere (Seinfeld and Pankow, 2003) would be
765 needed. The partitioning of phthalic acid into aerosol water cannot explain the mean f_{part} for
766 phthalic acid, based on its Henry's law constant of 2.0×10^{-11} atm m⁻³ mole⁻¹ (USEPA EPI suite)
767 and the assumption that the ratio of aerosol water content to the dry aerosol mass is one and all
768 aerosol water is available to take up phthalic acid. The dissociation of phthalic acid was also
769 considered, but the contribution due to its dissociation to its mean f_{part} was negligible even when
770 pH was estimated by neutralized inorganic ions without inclusion of other organic acids.

771 Moreover, the aerosol water content is unlikely to be that high at the average RH of 34% in the
772 atmosphere (Khlystov et al., 2005; Schuster et al., 2009; Engelhart et al., 2011). Therefore, there
773 must be at least an additional partitioning pathway whereby particle-phase phthalic acid is
774 formed.

775

776 We infer that a likely pathway for phthalic acid partitioning to particles is through its
777 reaction with gas-phase ammonia. This is supported by the presence of excess ammonium in the
778 particle phase indicated by the cation-to-anion ratio of inorganic species measured by HR-ToF-
779 AMS (Figure 3.4). Evidence for reactions between organic acids and gas-phase ammonia is
780 provided by Na et al. (2007), whose results showed that ammonia dramatically increased SOA
781 yields by reactions with organic acids in chamber experiments. Furthermore, the positive
782 correlation between gas-phase ammonia and f_{part} of phthalic acid (linear regression $R^2=0.8$
783 between average f_{part} and the ammonia concentration) supports the hypothesis that phthalic acid
784 partitioning to particles is through reactions with gas-phase ammonia (Figure 3.5).

785

786 Reactions with ammonia can convert phthalic acid into ammonium salts with the low
787 vapor pressures and subsequently favor its partitioning into particles. Subcooled vapor pressures
788 of the formed salts can be more than 100 times lower than that of phthalic acid, even if just the
789 monoammonium salt was formed (the subcooled vapor pressure drop is estimated based on the
790 vapor pressure drop of organic acids after forming ammonium salt from USEPA EPI suite).
791 Additional support needed for the presence of phthalic acid ammonium salts is that these salts
792 can be measured as phthalic acid by the TAG instrument using a thermal desorption technique to
793 extract collected organics. This support is given in Hajek et al. (1971) wherein the investigation

794 of the thermal decomposition of ammonium salt of isophthalic acid shows that simultaneous
795 release of both ammonia and isophthalic acid molecules from diammonium salts occurs without
796 dehydration or amide formation.

797

798 **3.3.3. 6, 10, 14-trimethyl-2-pentadecanone**

799 The mean f_{part} of 6, 10, 14-trimethylpentadecanone was 4 ± 2 %, similar to that of its
800 reference compound (*n*-heptadecane), suggesting that there is no reactive uptake of it on particles
801 during the campaign contrary to the observations of pinonaldehyde and phthalic acid. These
802 results are in agreement with previous studies on the gas/particle partitioning of ketones (Esteve
803 and Noziere, 2005; Kroll et al., 2005). Esteve and Noziere (2005) suggested that aldol
804 condensation was too slow to contribute significantly to SOA under atmospheric conditions.
805 Kroll et al. (2005) showed that ketones did not produce observable volume growth in the
806 presence of acidic seeds even with concentrations of over 500 ppb. Other measured compounds
807 with a ketone functional group in our study, such as benzophenone and 1-hydroxycyclohexy-
808 phenyl methanone, were also present primarily in the gas phase.

809

810 **3.4 Conclusions and Implications**

811 Measurements of organic compounds in both gas and particle phases improves our
812 understanding of SOA formation mechanisms in the atmosphere. Ketones observed in our study
813 were present predominantly in the gas phase, suggesting that observed reactive uptake to
814 aerosols does not occur and absorption into aerosols is the dominant pathway for them to
815 contribute to SOA in the atmosphere. While absorption of gas-phase phthalic acid into the

816 particles can contribute to observed particle-phase concentrations, the major pathway to form
817 particle-phase phthalic acid is likely attributed to reactions with gas-phase ammonia. This
818 mechanism is expected to cause high O/C ratios in ammonia enriched areas because reactions
819 with ammonia favor the uptake of carboxylic acids onto particles. Therefore, formation of
820 condensable salts can be a significant area of uncertainty for SOA formation in ammonia
821 enriched areas. Pinonaldehyde contributes to SOA through reactive uptake. The presence of
822 pinonaldehyde in the particle phase when inorganic acids were neutralized suggests that strong
823 acids are not required for occurrence of reaction uptake of pinonaldehyde beyond that predicted
824 by the gas/particle partitioning theory. The effect of aerosol acidity on the partitioning of
825 pinonaldehyde into particles observed in laboratory studies is not displayed by our observations
826 using the relationship between the cation-to-anion ratio and the particle-phase fraction of
827 pinonaldehyde. The relationship between particle-phase pinonaldehyde and RH suggests that
828 aerosol water content likely plays a significant role in the formation and accumulation of
829 particle-phase pinonaldehyde in the absence of inorganic acids, but it is not the primary one. Our
830 observations highlight that further studies are needed to examine the effects of RH and organic
831 acids on the reactive uptake of pinonaldehyde and other aldehydes on neutral seed particles.

832

833 In-situ measurements of both gas- and particle-phase organic compounds have clearly
834 shown that multiple gas/particle partitioning pathways occur in the atmosphere and other
835 gas/particle partitioning pathways significantly improve the SOA yields relative to absorptive
836 gas/particle partitioning. Our results show that the occurrence of reactive uptake of
837 pinonaldehyde into particles does not require the availability of inorganic acids and subsequently
838 imply that this pathway is likely widespread. However, the pathway of formation of condensable

839 salts indicated by our observations of the gas/particle partitioning of phthalic acid could be only
840 significant in ammonia-rich environments. Therefore, further in-situ, time-resolved
841 measurements of gas/particle partitioning covering more oxygenated organic compounds are
842 needed to investigate SOA formation in different areas and provide parameterization for
843 inclusion of these pathways in SOA models. Additionally, since our results show that each of
844 three SOA tracers investigated here has distinct pathways to partition to particles, multiple
845 tracers are needed in source apportionment models to adequately represent SOA formation.
846 However, these tracers are present in both gas and particle phases. As a result, it raises a concern
847 about the accuracy of the source apportionment models using these SOA tracers without
848 correcting for gas adsorption on the sampling substrates.

849

850

851

852 **3.5 Tables and Figures**

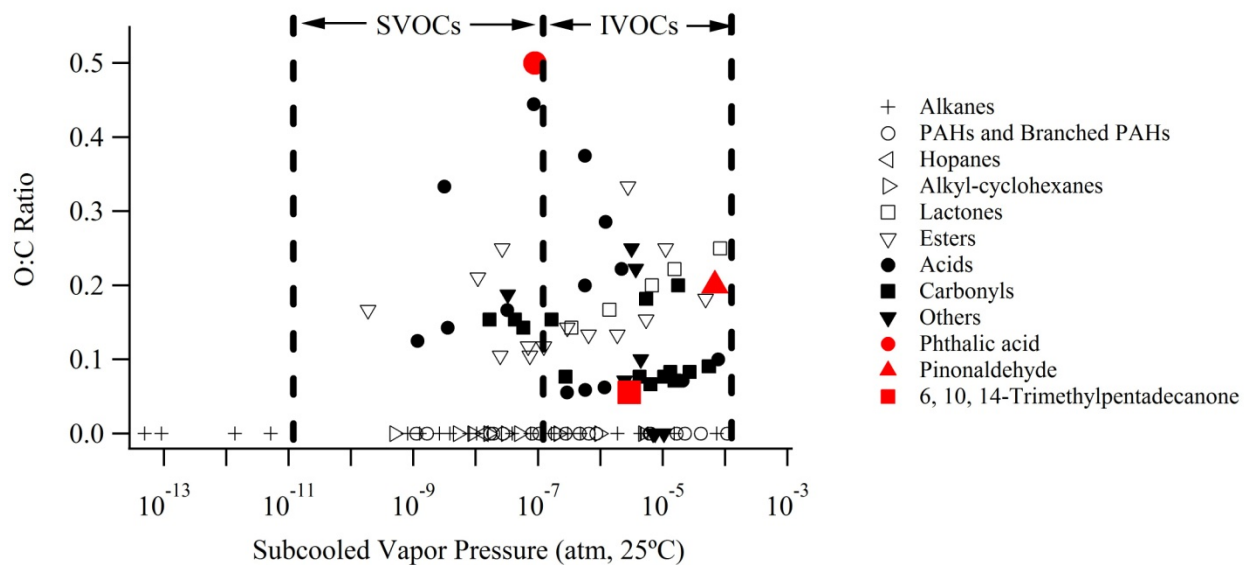
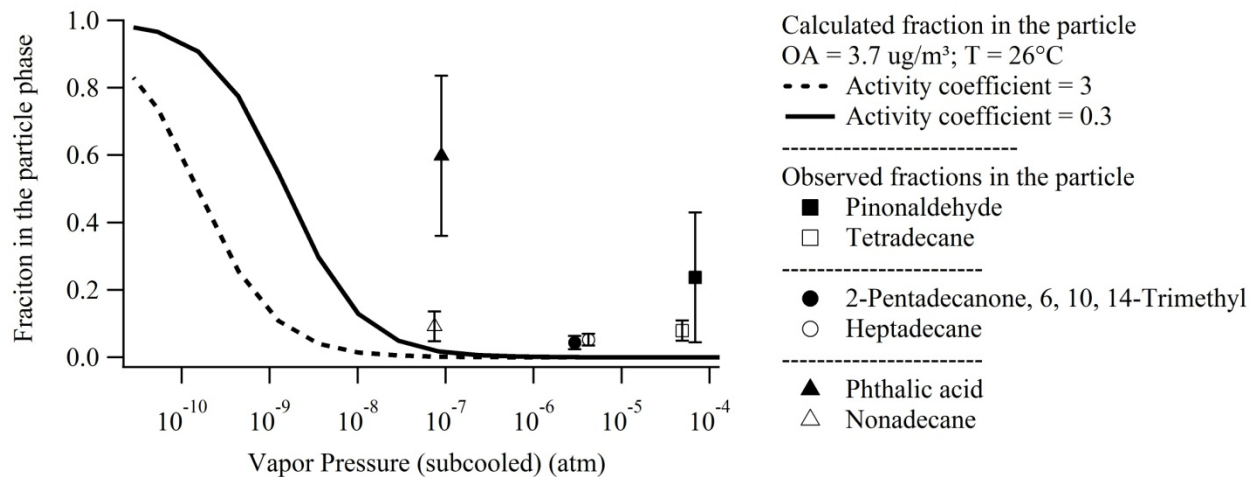


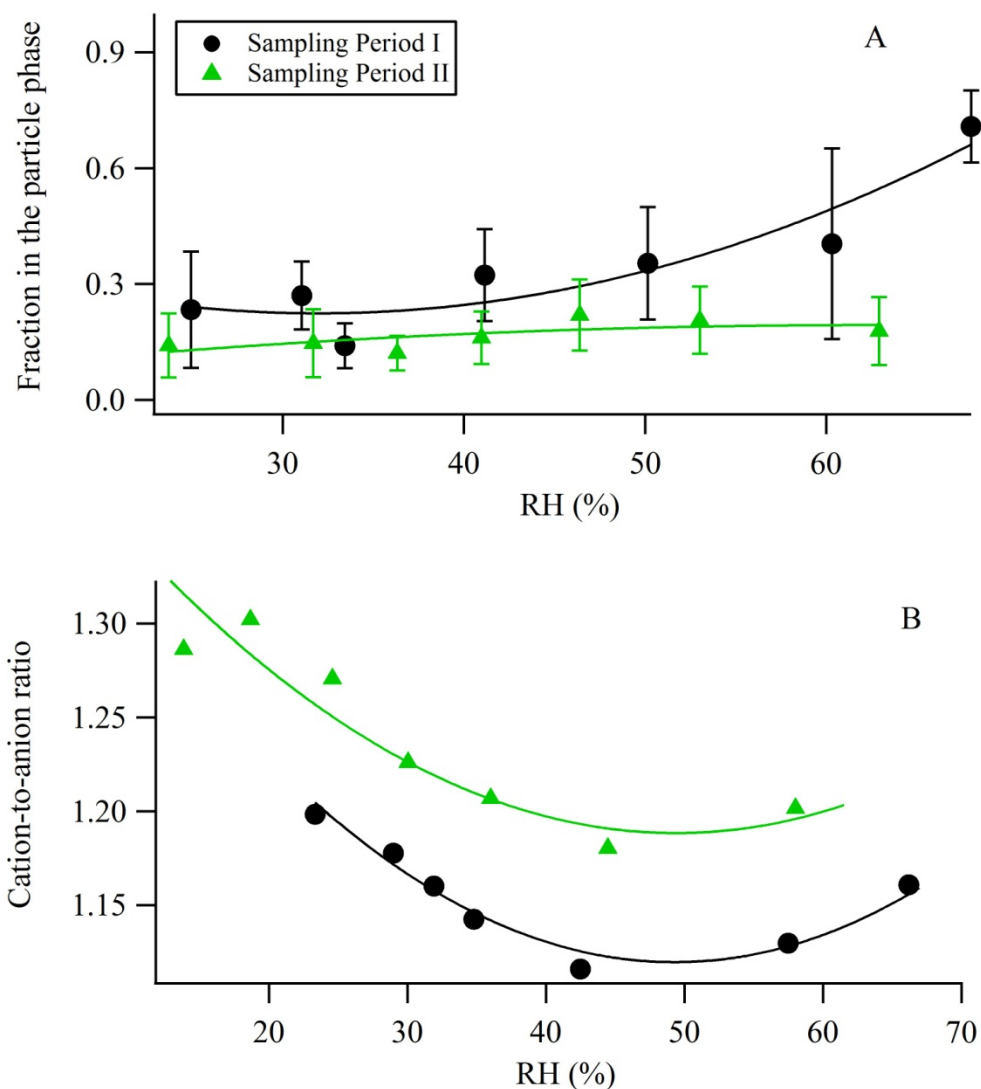
Fig. 3.1 O/C ratios of organic compounds measured by TAG as a function of subcooled vapor pressure at 25°C. The compounds of interest are colored in red.

858
859

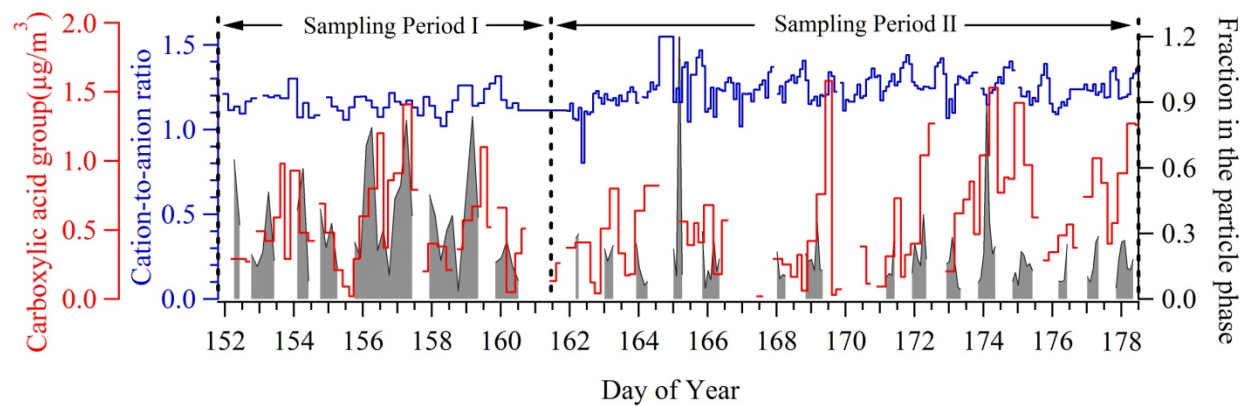


860
861
862
863
864
865
866

Fig. 3.2 Average measured fractions for selected oxygenated organic compounds (solid markers) and their corresponding reference compounds (empty markers). The vertical bars are one standard deviation of the mean. The solid and dashed lines are the predicted fraction of organic compounds in the particle phase with different vapor pressures using equations 3.2 and 3.3.

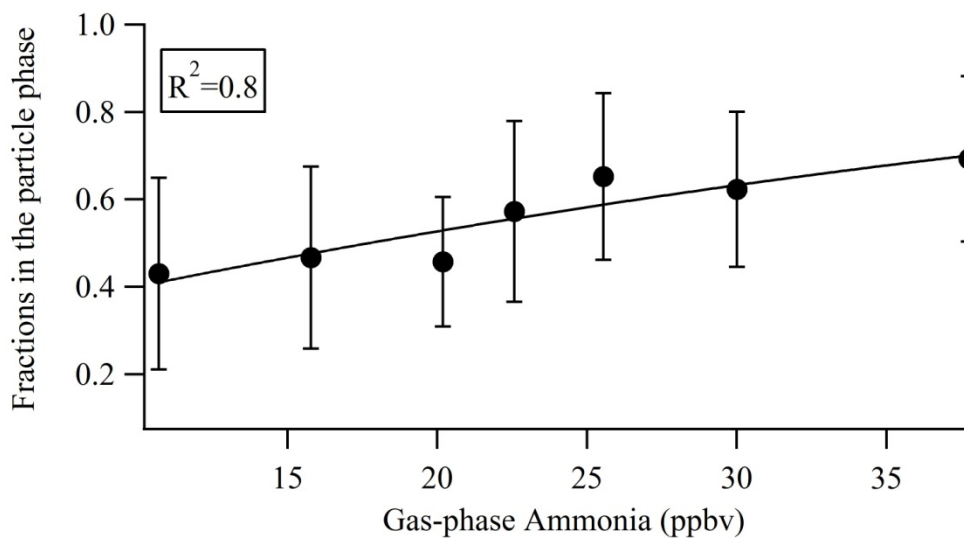


867
 868
 869
 870 **Fig. 3.3 A)** Measured fraction of pinonaldehyde in the particle phase as a function of RH
 871 (average 5 or 6 points in each bin in Sampling Period I; 12 points in each bin in Sampling Period
 872 II). The error bar is one standard deviation of the mean. The X-axis value is the average value of
 873 RH in each bin. Fractions larger than 3 standard deviations outside of the mean in each sampling
 874 period are considered outliers and excluded in this plot. B) The average cation-to-anion ratio of
 875 inorganic species (sulfate, nitrate and ammonium) as a function of RH (average 7 points in each
 876 bin in Sampling Period I; 27 points in each bin in Sampling Period II).
 877



878
 879 **Fig. 3.4** The temporal change of the cation-to-anion ratio of measured inorganic ions, carboxylic
 880 acid group and the fraction of pinonaldehyde in the particle phase.
 881
 882
 883

884



885

886

887

888

889

890

Fig. 3.5 Fraction of phthalic acid in the particle phase as a function of the concentration of gas-phase ammonia. Each bin of seven bins has 18 data points.

891

892

893

894

895

896

897

898

899

900

901

902

903

904 **4. Sources of organic aerosol investigated using organic** 905 **compounds as tracers measured during CalNex Bakersfield**

906

907

908 **4.1 Introduction**

909 Organic compounds constitute a major mass fraction (20-90%) of atmospheric fine
910 particulate matter in most environments (Kanakidou et al., 2005). These organic compounds
911 have been categorized into either primary organic aerosol (POA), directly emitted from various
912 primary sources such as food cooking and vehicle exhausts (e.g. Schauer et al. 1999a, b, 2002a),
913 or secondary organic aerosol (SOA), formed in the atmosphere through chemical reactions
914 (Odum et al., 1997; Jang et al., 2002; Robinson et al., 2007; Kroll and Seinfeld, 2008). The
915 majority of organic aerosol (OA) in rural and urban areas is secondary (Zhang et al., 2007;
916 Shrivastava et al., 2007; Williams et al., 2010; Jimenez et al., 2009). SOA and POA have been
917 shown to have different adverse effects on human health (Li et al., 2009), so quantifying source
918 contributions to OA has important implications for air quality regulation.

919

920 Source apportionment between POA and SOA has generally been done in one of three
921 ways; (i) bulk organic spectra measured by the Aerodyne Aerosol Mass Spectrometer (e.g.
922 Jimenez et al., 2009; Zhang et al., 2011), (ii) thermal-optical elemental carbon/organic carbon
923 analyzer (e.g. Turpin et al., 1991; Strader et al., 1999) and (iii) molecular speciation measured by
924 gas chromatograph/mass spectrometer (GC/MS) (e.g. Shrivastava et al., 2007; Williams et al.,
925 2010). In comparison with bulk organic analysis, the molecular speciation resolves a smaller
926 fraction of OA, but the identified organic compounds can serve as tracers for specific source
927 types (Schauer et al., 1996; Schauer and Cass, 2000) and provide information for understanding

928 SOA formation and transformation in the atmosphere (e.g. Kleindienst et al., 2007; Williams et
929 al., 2010). Two common source apportionment methods using organic compounds are the
930 chemical mass balance (CMB) and positive matrix factorization (PMF) models (e.g. Schauer et
931 al., 1996; Shrivastava et al., 2007; Williams et al., 2010).

932

933 The CMB model uses organic compounds to estimate OA contributions from a variety of
934 sources, such as biomass burning, meat cooking, or diesel vehicle emissions, but requires *a*
935 *priori* knowledge of their source profiles as inputs to solve the model (Schauer et al., 1996;
936 Schauer and Cass, 2000; Zheng et al., 2002). As a result, CMB analysis is sensitive to the
937 provided source profiles (Robinson et al., 2006; Subramanian et al., 2007). The products and
938 SOA yields measured for a few known volatile organic compounds (VOCs) oxidized in chamber
939 experiments have been considered as source profiles of SOA (Kleindienst et al., 2007; Stone et
940 al., 2009). However, the relevance of these source profiles is limited to these known compounds
941 and the specific experimental conditions used in the chamber to derive the profiles. Source
942 profiles for SOA are difficult to establish due to the complexity of oxidation processes and the
943 wide range of precursors and atmospheric conditions, so CMB models have typically been
944 unable to provide adequate constraints on the SOA mass or composition. Though SOA mass can
945 be estimated by CMB models as the difference between apportioned OA and measured OA, they
946 do not provide detailed information about SOA sources (Schauer et al., 1996; Zheng et al., 2002;
947 Subramanian et al., 2007).

948

949 The PMF model uses covariation between organic compounds to categorize them into
950 unique groups or factors that could represent emissions from contemporaneous source or

951 formation processes (Shrivastava et al., 2007; Zhang et al., 2009; Williams et al., 2010). Since *a*
952 *priori* knowledge of source profiles is not required, factors likely representing poorly
953 constrained or unknown sources, such as SOA, can be determined. Characterization of these
954 factors based on their compositions and temporal variations therefore provide an effective tool
955 for differentiating complex sources (Shrivastava et al., 2007; Zhang et al., 2009; Williams et al.,
956 2010). Past work has demonstrated the ability of this method to separate multiple SOA types
957 with distinct diurnal patterns in the absence of known source profiles (Williams et al., 2010).
958 Despite its utility for source apportionment, PMF analysis is not widely performed on organic
959 compounds in the particle phase because it typically requires a larger number of samples which
960 poses significant challenges when measurements of speciated OA are mainly made by filter
961 sampling with 24-hour collection periods in the field followed by solvent extraction in the
962 laboratory for analysis (Jaeckels et al., 2007; Shrivastava et al., 2007). Recently, speciated
963 measurements of OA have been facilitated by the development of an in-situ Thermal desorption
964 Aerosol Gas chromatography instrument (TAG) which provides hourly time resolved chemical
965 speciation of OA (Williams et al., 2006). As a result of the hourly time resolution, the TAG
966 provides as many data points in a few weeks of measurements as solvent extracted filters are able
967 to in a year, thus enabling multivariate statistical analyses. TAG data have been analyzed by
968 PMF in previous work to resolve nine different types of OA in an urban environment, including
969 various SOA and POA sources (Williams et al., 2010).

970

971 In this work, we focus on data from a field site in Bakersfield, CA, one of two supersites
972 of the CALifornia at the NEXus between Air Quality and Climate Change (CalNex) campaign in
973 June 2010. Previous studies of source contributions to OA in the Bakersfield area were based on

974 the EC-tracer method and CMB and focused on OA in winter (Magliano et al., 1999; Strader et
975 al., 1999; Schauer et al., 2000). Neither the EC-tracer method nor CMB was able to provide
976 insights into different SOA types. In this study, we perform PMF analysis on TAG data from
977 Bakersfield, CA to investigate source contributions to OA in June, including primary emissions
978 and atmospheric processes to form SOA. Factors determined by PMF analysis are associated
979 with specific source types and atmospheric processes based on measured organic compounds in
980 the context of an urban area and the agricultural, natural, and industrial sources present in the
981 region.

982

983 **4.2 Methods**

984 **4.2.1 Sampling and Chemical Analysis**

985 Speciated measurements of particle-phase organics were made with the TAG instrument
986 during the CalNex field campaign from May 31st to June 27th 2010 at the Bakersfield supersite,
987 CA. A description of the TAG is provided by Williams et al. (2006), and details on updates and
988 operation of the TAG used in this work are provided in Zhao et al. (2012). Briefly, the TAG was
989 updated by addition of a denuder into the sampling inlet so that there were two parallel sampling
990 lines, one denuder line and one bypass (no denuder) line made of stainless steel tubing. During
991 sampling, ambient air was pulled at 10 L/min through a PM_{2.5} cyclone from the center of a main
992 sampling flow of 200 L/min drawn from ~5 meters above the ground through a 6-inch i.d. rigid
993 duct and gas- and particle-phase organics were collected by an impactor. The sampling flow was
994 alternated between the denuder line to collect only particle-phase organics, and the bypass line to
995 collect total organics, the sum of gas- and particle-phase organics. Following sampling, the
996 collected organics were thermally desorbed and injected into a gas chromatograph-mass
997 spectrometer (GC/MS) for analysis. Identification and quantification were achieved using a

998 quadrupole mass spectrometer (Agilent, 5973) calibrated based on responses to authentic
999 standards that were manually injected into the impactor cell at regular intervals throughout the
1000 campaign (Kreisberg et al., 2009). During this campaign, TAG measurements were made in two
1001 periods wherein the sampling durations were different. The duration of each sample was 90
1002 minutes from May 31st to June 9th (Sampling period I) and 30 minutes from June 10th to 27th
1003 (Sampling period II). Over the 27-days of measurements, 244 samples of speciated OA were
1004 acquired and over 100 particle-phase organic compounds were identified and quantified.

1005
1006 Supporting measurements conducted concurrently that are relevant to data analysis and
1007 discussion in this study included detailed characterization of meteorological conditions, OA, and
1008 volatile organic compounds (VOCs). Wind speed and direction were monitored by a propeller
1009 wind monitor (R.M. Young, 5130). Details on measurements of submicron OA made with an
1010 Aerodyne High-Resolution Time-of-Flight Aerosol Mass Spectrometer (HR-ToF-AMS) are
1011 provided in Liu et al., (2012). Gas-phase VOCs were measured by an automated in-situ GC-
1012 FID/MS system (Gentner et al., 2012). In addition, ozone was measured using a UV photometric
1013 ozone analyzer (Dasibi Inc., model 1008 RS).

1014

1015 **4.2.2 PMF Procedures**

1016 The positive matrix factorization (PMF) model describes observed concentrations of
1017 organic species as the linear combination of the contributions from a number of sources with
1018 constant profiles (Paatero and Tapper, 1993; Hopke, 2003; Reff et al., 2007; Ulbrich et al.,
1019 2009):

$$1020 \quad x_{ij} = \sum_p g_{ip} f_{pj} + e_{ij} \quad (4.1)$$

1021 where x_{ij} is the concentration of species j measured in sample i , g_{ip} is the contribution of factor p
1022 to sample i , f_{pj} is the concentration of species j in factor p and e_{ij} is the residual not fit by the
1023 model. PMF solves the equations for g_{ip} and f_{pj} to best reproduce x_{ij} without *a priori* knowledge
1024 of them based on the selected number of factors (p). The solution to PMF minimizes the object
1025 function, Q , defined as:

$$1026 \quad Q = \sum_{i=1}^n \sum_{j=1}^m \left(\frac{e_{ij}}{s_{ij}} \right)^2 \quad (4.2)$$

1027 where s_{ij} is the estimated uncertainty of species j measured in sample i .

1028

1029 As the PMF model allows each data point to be individually weighted, the uncertainties
1030 associated with organic compounds at different concentration levels are estimated separately. By
1031 estimating the uncertainty using this approach, missing data points can be weighted, so
1032 compounds or days with many missing points do not need to be removed. This approach
1033 provides an advantage over many other methods by achieving longer timelines of observations
1034 (Pollissar et al., 1998). In our study, data points, which were not detected because of low
1035 concentration, were assigned a concentration of one third of the compounds detection limit, and
1036 uncertainty was assigned to be four times its concentration, similar to the estimation made in
1037 Pollissar et al. (1998). The uncertainty for the measured data point was estimated using the same
1038 equations described in Williams et al. (2010). In contrast to that work, however, the detection
1039 limit of each compound was used in the current study to better account for the instrument noise,
1040 instead of instrument precision derived from the standard deviation of the difference between
1041 consecutive data points used in Williams et al., (2010).

1042

1043 To investigate the major OA sources in this study, only the particle-phase organics were
1044 included in the PMF analysis. In the Appendix B, we demonstrated that the inclusion of gas-
1045 phase contributions to semi-volatile organic compounds (SVOCs) significantly bias the results of
1046 source apportionment. The criteria we used for inclusion of compounds were that the timeline of
1047 observations covered the entire period of TAG measurements, the compounds were in the
1048 particle phase, and the percentage of above detection limit data points was greater than 50% over
1049 the full timeline of observations. As a result, 30 compounds (listed in Figure 4.1) in 244 samples
1050 were included in the PMF analysis. PMF was applied using the Igor based PMF Evaluation Panel
1051 v2.04 (Ulbrich et al., 2009).

1052

1053 Detailed discussions of determination of the optimum number of PMF factors can be
1054 found in the literature of Reff et al. (2007), Ulbrich et al. (2009) and Williams et al. (2010), and
1055 interpretability of these factors is an important criterion. In our study, the linkage between factors
1056 and specific OA source types or atmospheric processes was initially made based on the existing
1057 knowledge of specific sources of individual compounds in each factor and was further
1058 corroborated by their diurnal profiles and supporting measurements, such as VOCs and
1059 meteorological conditions.

1060

1061 Although the sum of concentrations of all species included in PMF analysis accounts for
1062 only a small fraction of AMS measured OA, the mass contribution of each factor to measured
1063 OA can be calculated by a multivariate fit of the temporal contributions of PMF factors onto total
1064 AMS measured OA mass concentrations (Reff et al., 2007; Williams et al., 2010). The sum of
1065 these calculated mass contributions are defined as reconstructed OA. The regression coefficients

1066 for factors provide an additional constraint on the number of factors to be included, since
1067 negative regression coefficients are a good indication that the number of factors exceeds the
1068 optimum (Reff et al., 2007).

1069

1070 **4.3 PMF Results**

1071 The variability of the TAG data is best explained by six factors with a value of $Q/Q_{expected}$
1072 equal to 2.5 with F_{peak} set to 0. Since the interpretability is an important criterion in determining
1073 the optimal number of factors, 5-factor and 7-factor solutions were also explored. In comparison
1074 with the 6-factor solution, the 5-factor solution resulted in a convolution of factors 1 and 5. The
1075 7-factor solution split factor 6, which is a mixture of anthropogenic and biogenic SOA factors,
1076 without providing additional meaningful information. We therefore chose to examine the 6-
1077 factor solution in detail to characterize the major components of total OA. To facilitate
1078 discussion, we define 8:00-20:00 PST as the day and 20:00-8:00 PST as the night.

1079

1080 **4.3.1 Factor 1: Local POA**

1081 We define factor 1 as local POA. Factor 1 has the highest contribution from
1082 hydrocarbons among the six factors (Figure 4.1) and has a diurnal profile with higher
1083 concentrations at night, consistent with buildup of local emissions into a shallow nighttime
1084 boundary layer (Figure 4.2). Highest concentrations of this factors occurred during the night, at
1085 low wind speeds, and with wind coming from all directions (Figures 4.2 and 4.3) indicating that
1086 it originated mainly from local sources because Bakersfield is located near the southern end of
1087 the San Joaquin Valley. One of the two main oxygenated compounds present in this factor was
1088 9-fluorenone, which has been identified as a primary emission from motor vehicles (Schauer et

1089 al., 1999). The other prominent oxygenated compound present in this factor was phthalic acid.
1090 Phthalic acid is produced from oxidation of naphthalene and has been used as a tracer for
1091 anthropogenic SOA (Schauer et al., 2002b; Fine et al., 2004; Shrivastava et al., 2007), but its
1092 average concentration in this factor accounts for less than 1% of its total measured concentration
1093 so we consider this a very minor contribution of SOA adding to this POA dominated factor.

1094
1095 The major known POA sources in Bakersfield are wood burning, meat cooking and
1096 motor vehicles (Schauer et al., 2000) and the average contribution of unknown POA sources to
1097 OA was small (~10%) (Schauer et al., 2000; Strader et al., 1999). Our POA factor correlated
1098 with several measured hopanes ($r > 0.54$), which were not included in the PMF analysis because
1099 over 50% of their data points were below detection limit. The good correlations with hopanes
1100 suggest that this factor is mainly related to motor vehicles that have been identified as the
1101 dominant source of hopanes in urban environments (Schauer et al., 1996; 2002; Schauer and
1102 Cass, 2000). Tracers for meat cooking, such as palmitoleic acid and cholesterol, were not
1103 detected and the detected tracer for wood burning, retene, was only observed in a few particle-
1104 phase samples.

1105

1106 **4.3.2 Factor 2: A mixture of OA sources**

1107 We define factor 2 as a mixture of OA sources with contributions from both POA and
1108 SOA. While hydrocarbons accounted for a significant fraction of this factor, relative to local
1109 POA there was a smaller fraction of each PAH and a larger fraction of each phthalate (Figure
1110 4.1). Additionally, an SOA tracer, 6, 10, 14-methyl-2-pentadecanone (Shrivastava et al., 2007),
1111 apparently contributed to this factor, relative to the POA factor wherein this tracer was not

1112 present. The composition of this factor suggests that it was affected by a variety of different
1113 sources and atmospheric chemical processes. The large difference in the concentration range in
1114 alternating intervals of its 2-hr diurnal profile is caused by very different concentrations observed
1115 during two sampling periods. The concentrations in Sampling Period I were higher than those in
1116 Sampling Period II and were plotted in every other sampling interval. The diurnal profile for the
1117 concentration of this factor was examined separately for each sampling period, but neither period
1118 had a clear diurnal cycle, suggesting again that this factor is mostly likely a mixture of OA
1119 sources.

1120

1121 **4.3.3 Factors 3 : SOA1**

1122 We define factor 3 as SOA1. The contribution of organic species to this factor was
1123 dominated by oxygenated compounds (Figure 4.1). Methyl phthalic acid has been used as a
1124 tracer for anthropogenic SOA (Fine et al., 2004; Williams et al., 2010) and 9,10-anthraquinone
1125 has been observed as oxidation products of PAHs (Helmig et al., 1992; Helmig and Harger,
1126 1994). The elevated concentration of this factor during 20:00-24:00 PST (Figure 4.2) is
1127 attributed to the low wind speed and low temperature, which favors the accumulation of gas-
1128 phase oxygenated compounds in the afternoon and subsequent condensation of them onto
1129 particles to contribute to SOA. These condensable oxygenated compounds can be formed locally,
1130 and probably include some organic nitrates (Rollins et al., 2012), and can also be produced
1131 upwind and transported to the site during the afternoon along with SOA3 (discussed below).

1132

1133 **4.3.4 Factor 4: SOA2**

1134 We define factor 4 as SOA2. The dominant contribution of organic species to this factor
1135 was from two SOA tracers, phthalic acid and methyl-phthalic acid, though other compounds,
1136 both hydrocarbons and oxygenated compounds, were present but with much smaller
1137 contributions. Evidence that this factor was associated with photochemically produced SOA is
1138 apparent when comparing the diurnal profile of this factor with that of the ratio of 1,3,5-
1139 trimenthylbenzene (TMB) to toluene. Because both 1,3,5-TMB and toluene have similar source
1140 types in Bakersfield (Gentner et al., 2012) and 1,3,5-TMB reacts faster with OH radicals than
1141 toluene does (Atkinson and Arey, 2003), a smaller ratio of 1,3,5-TMB to toluene indicates that
1142 the air mass is more oxidized. An opposite trend between the average diurnal profile of this
1143 factor and that of the ratio of 1,3,5-TMB to toluene clearly shows that higher concentrations of
1144 this factor occurred when gas-phase organics were more oxidized (Figure 4.2). The highest
1145 concentration of this factor occurred in the morning (8:00-9:00 PST) when the wind speed was
1146 low (Figure 4.2), indicating that this SOA was formed locally.

1147

1148 **4.3.5 Factor 5: SOA3**

1149 We define factor 5 as SOA3. This factor had the highest concentrations in the afternoon
1150 (Figure 4.2) and correlated with ozone ($r=0.62$). The dominant contribution of organic species to
1151 this factor was from oxygenated compounds (Figure 4.1). However, the diurnal patterns of the
1152 ratio of 1,3,5-TMB to toluene did not correlate well with this factor, especially in the afternoon
1153 (Figure 4.2). The afternoon ratio of 1,3,5-TMB to toluene was close to the nighttime ratio,
1154 indicating that observed VOCs were fresh and emitted locally without having undergone
1155 significant oxidation. Therefore, we infer that SOA in this factor was not formed through local
1156 VOC oxidation, but instead was composed primarily of regionally formed, transported SOA.

1157 This inference is supported by relatively high wind speeds (from the northeast) during the
1158 observations of high concentrations of this factor (Figure 4.3) would carry regional source
1159 contributions to the observation site, but would dilute local source contributions.

1160

1161 **4.3.6 Factor 6: Nighttime SOA (SOA4)**

1162 We define factor 6 as nighttime SOA (SOA4). This factor had the highest concentrations
1163 at night with the dominant contribution from SOA tracers phthalic acid, methyl phthalic acid, 6,
1164 10, 14-methyl-2-pentadecanone and pinonaldehyde. Pinonaldehyde is a volatile oxidation
1165 product of a biogenic VOC, α -pinene, and can contribute to SOA by forming low vapor pressure
1166 products, such as dimers (Tolocka et al., 2004; Liggió and Li, 2006). The factors controlling
1167 gas/particle partitioning of pinonaldehyde at this site has been analyzed in a separate paper (Zhao
1168 et al., 2012). Deconvolution of biogenic and anthropogenic contributions is difficult due to the
1169 co-variation of chemical transformations leading to SOA, but it is evident that SOA from
1170 biogenic VOC oxidation contributed significantly to SOA4 as the highest concentrations of this
1171 factor were most frequently observed when the wind blew from the vegetated areas located to the
1172 east of the field site (Figure 4.3).

1173

1174 **4.4 Reconstructed OA**

1175 Reconstructed OA based on TAG-derived factors was compared with measured OA to
1176 evaluate the capability of the TAG-derived factors to capture the variability of AMS measured
1177 OA. Good agreement between the reconstructed and measured OA was demonstrated, with
1178 differences between them of less than 20% for over 70% of observations (Figure A1a). The
1179 reconstructed OA had largest uncertainties at the lowest measured OA concentrations and was

1180 generally lower than the measured OA at high measured OA concentrations. This could be
1181 attributed to larger uncertainties related to organic species when the atmospheric OA
1182 concentration was low and lack of inclusion of additional organic tracers in the current dataset
1183 when the atmospheric OA concentration was high (because they were below detection limit in
1184 more than 50% of observations or cannot be measured by TAG). As shown by Figure A1b, the
1185 negative relative residuals mainly occurred at night. One reason for these negative residuals
1186 could be that the TAG did not measure a tracer for organic nitrates which have been shown to
1187 significantly contribute to nighttime OA in this region (Rollins et al., 2012).

1188

1189 **4.5 Source contributions to OA mass**

1190 The local POA source accounted for an average 15% of total OA and motor vehicles
1191 were shown to have a significant contribution to local POA. The average contribution of POA to
1192 total OA could be up to 28% if we assumed that all of the mass of the mixture of OA sources is
1193 POA, but this is surely an overestimate. The contributions from other specific primary sources
1194 cannot be determined individually in this study because they are small and PMF analysis cannot
1195 reliably separate very small factors among the noise and variation of the larger factors. The
1196 emissions in the Bakersfield region are highly complex with cars, trucks, oil and gas extraction
1197 and refining operations, agricultural activities and other sources all potentially contributing some
1198 to these POA factors. The average contribution of the sum of SOA (SOA 1-4) was 72% of total
1199 OA and the contribution of SOA could be up to 85% if the mass in the mixture of OA sources is
1200 only considered as SOA. The dominance of SOA in total OA derived from organic species in
1201 this study is consistent with the results reported by Liu et al. (2012) based on PMF analysis of
1202 AMS observations from the same site which showed that 80% to 90% of total OA is accounted

1203 for by SOA. We conclude that efforts to control atmospheric OA in this region must focus on
1204 understanding and then controlling the sources of SOA precursors or factors leading their
1205 transformation into SOA.

1206
1207 We calculated the diurnal cycle of relative contribution from each identified component
1208 to OA (Figure 4.4) to highlight the dominant components of OA in different periods of the day
1209 and night. The factors contributing the largest fraction of total OA was different during the day
1210 and night, but both of them were SOA. The largest daytime contribution to total OA was from
1211 regional SOA formation (SOA3), and this factor accounted for ~50% of total OA throughout the
1212 day. The nighttime SOA factor (SOA4) accounted for 39% of total OA at night, but provided
1213 only a very small contribution to total OA during the day. The more local SOA factor (SOA2)
1214 also contributed substantially to total OA, accounting for 21% of the total OA when it reached its
1215 highest concentration in the morning (8:00 - 12:00 (PST)). The smaller local SOA factor (SOA1)
1216 accounted for < 10% of total OA during all periods of the day. Both local (SOA2) and regional
1217 (SOA3) significantly contributed to total OA (12~21% and 40~56%, respectively) during the
1218 day. We conclude that control of SOA precursor emissions on both local and regional scales
1219 should reduce the daytime OA concentration, with the dominant contribution being regional.

1220

1221 **4.6 Formation Pathways of SOA**

1222 Controlling emissions of pollutants involved in the formation pathways of SOA has the
1223 potential to play a significant role in reducing regional OA concentrations (e.g. Liggió and Li,
1224 2006; Na et al., 2007). In areas where biogenic emissions are oxidized in the presence of
1225 anthropogenic pollutants such as SO₂, NO_x and black carbon, it has become increasingly

1226 apparent that SOA formation from biogenic VOC is substantially enhanced (Goldstein et al.,
1227 2009; Surratt et al., 2010; Carlton et al., 2010; Spracklen et al., 2011). Rollins et al. (2012) has
1228 shown that in the Bakersfield region reductions in NO_x can reduce the OA concentration because
1229 of the involvement of NO_x in formation of organic nitrates. Here we suggest that TAG-derived
1230 factors can be indicative of the dominant formation pathway for each SOA type identified. The
1231 pathways of oxygenated compounds contributing to SOA in each factor can be used to draw a
1232 distinction between direct gas-to-particle condensation wherein oxidation reactions produce low
1233 volatility products that condense, secondary gas-to-particle condensation wherein non-oxidation
1234 reactions produce lower volatility products that condense, such as reactions between carboxylic
1235 acids and ammonia, and reactive uptake wherein compounds expected to be in the gas-phase
1236 enter the particle phase through acid-catalyzed reactions. Evidence for these formation pathways
1237 in Bakersfield during CalNex based on individual compounds – specifically phthalic acid,
1238 pinonaldehyde and 6, 10, 14-trimethyl-2-pentadecanone has been explored and reported by Zhao
1239 et al. (2012). Ketones enter the particle phase primarily through direct gas-to-particle
1240 condensation, while phthalic acid was shown to enter the particle phase mainly through reaction
1241 with ammonia in the gas phase (Zhao et al., 2012). It is likely that SOA1 and SOA3 were formed
1242 at least partially by direct gas-to-particle condensation because the dominant contribution to the
1243 factor profiles of these two factors are from compounds with ketone functional groups. The
1244 factor profile of SOA2 is primarily determined by particle-phase phthalic acid formed through
1245 reactions with gas-phase ammonia, indicating the reactions of carboxylic acids and ammonia
1246 play a significant role in the formation of SOA2. This formation pathway is also supported by
1247 the strong correlation ($r > 0.5$) between the concentration of SOA2 and the concentration of excess
1248 ammonium calculated using ammonium, sulfate and nitrate measured AMS. This formation

1249 pathway could be site-specific because it needs excess ammonia to allow these reactions with
1250 carboxylic acids to occur. For SOA4 (i.e., the nighttime SOA) the factor profile contains
1251 pinonaldehyde, as well as phthalic acid and 6, 10, 14-2-pentadecanone. The presence of
1252 pinonaldehyde in the particles indicates the occurrence of acid-catalyzed reactions in the
1253 particles (Zhao et al. 2012). However, the relative contribution to the nighttime OA from these
1254 particle-phase reactions with acids cannot be distinguished from the direct gas-to-particle
1255 condensation. Zhao et al. (2012) has shown that secondary gas-to-particle partitioning and
1256 reactive uptake can significantly increase SOA yields of phthalic acid and pinonaldehyde relative
1257 to direct gas-to-particle partitioning. Therefore, control of species involved in these pathways of
1258 gas-to-particle partitioning such as ammonia and organic acids could also lead to reductions in
1259 the OA concentration, in addition to control of organic precursors. However, the efficiency of
1260 reduction of SOA concentrations by control ammonia needs further investigation. For example,
1261 the reduction of ammonia would increase the aerosol acidity which could increase the SOA
1262 formation from particle-phase reactions (Jang et al., 2002; Liggió and Li, 2006).

1263
1264 To substantiate that the formation pathways of SOA can be indicated by individual
1265 compounds, daytime SOA types derived from PMF analysis of organic species were compared to
1266 those from PMF analysis of bulk organic mass spectra measured by AMS (Figure 4.5). The
1267 contribution of the daytime SOA (the sum of SOA2 and SOA3) derived from organic species to
1268 total OA in this study displays a similar diurnal profile to SOA of the sum of high O/C alkane
1269 (O/C=0.68), high O/C aromatic (O/C=0.63) and petroleum (O/C=0.20) SOA derived from AMS
1270 mass spectra reported in Liu et al. (2012) from the same measurement campaign, which were
1271 selected because their mass fraction exhibited a daytime enhancement. The consistency of

1272 daytime SOA between these two studies supports that oxygenated organic compounds observed
1273 by TAG are able to reproduce the trend of SOA formation during the day.

1274

1275 **4.7 Conclusions and Atmospheric Implications**

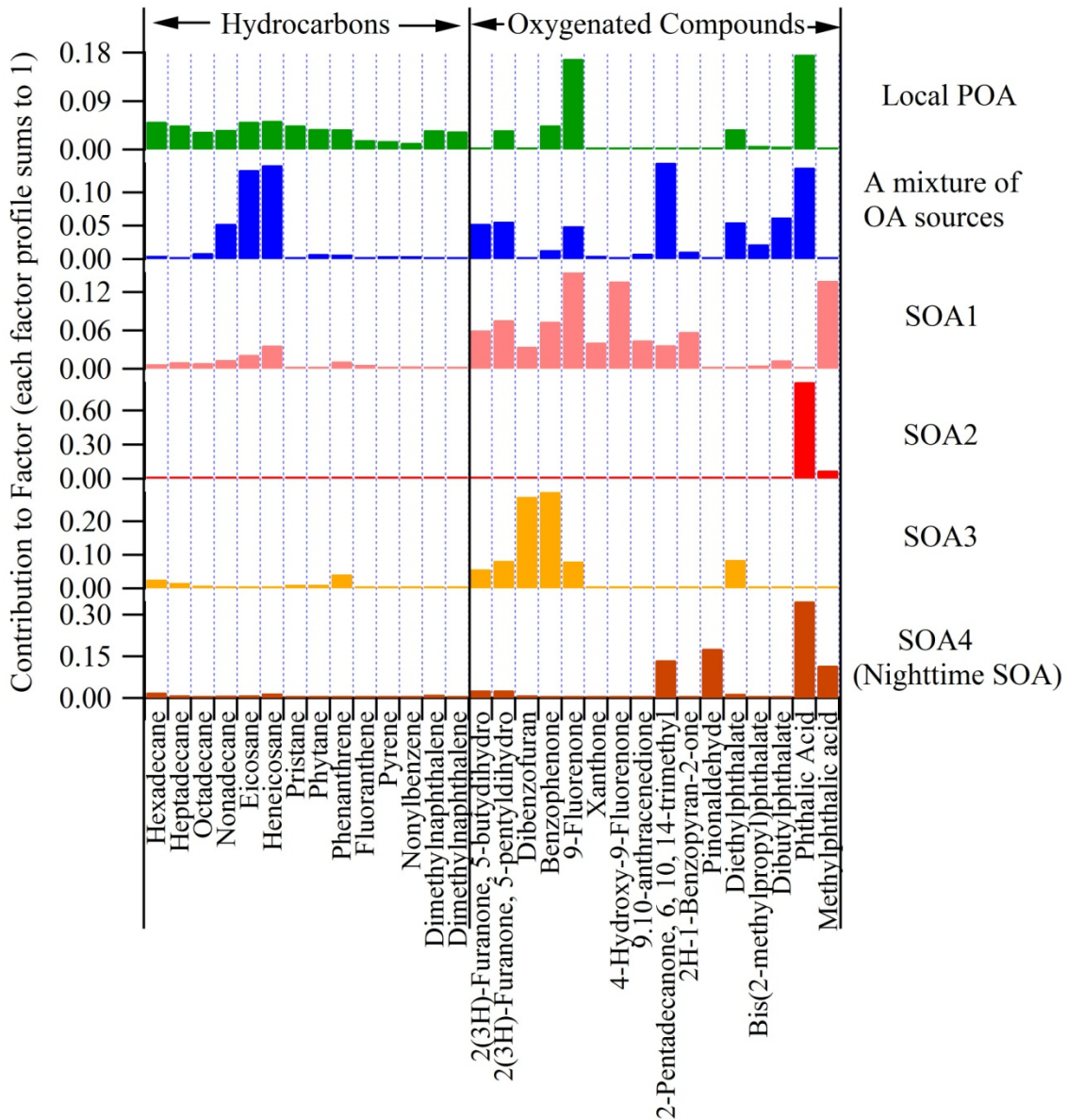
1276 PMF analysis was performed on 244 particle-phase speciated organic samples, acquired
1277 over a month, to investigate OA sources. The variability of this dataset was best explained by six
1278 types of OA sources using PMF analysis. The concentration of reconstructed OA based on these
1279 six factors was in good agreement with the concentration of measured OA. Local POA
1280 accounted for 15% of the total OA on average and is suggested to be mostly contributed by
1281 motor vehicles. SOA was the dominant component of total OA throughout the day and night.
1282 SOA (the sum of SOA1-4) accounted for an average 72% of total OA with an average diurnal
1283 variation in the range from 66% at night to 78% during the day. Regional SOA (SOA3, 56%)
1284 was dominant during the afternoon and nighttime SOA (SOA4, 39%) was dominant during the
1285 night. Local SOA (SOA2) contributed significantly in the morning, accounting for 21% of total
1286 OA in the morning (from 8:00 am to 12:00 pm PST).

1287

1288 Our results suggest that the formation of SOA in this study occurred through multiple
1289 pathways, some of which may be regionally-specific due to the unique mixture of emissions in
1290 this airshed. SOA, including SOA1 and SOA3, formed dominantly through direct gas-to-particle
1291 condensation. Secondary gas-to-particle partitioning also played major role in formation of local
1292 SOA (SOA2). Particle-phase reactions also contributed to formation of nighttime SOA (SOA4),
1293 but their contributions are not well-constrained in this study.

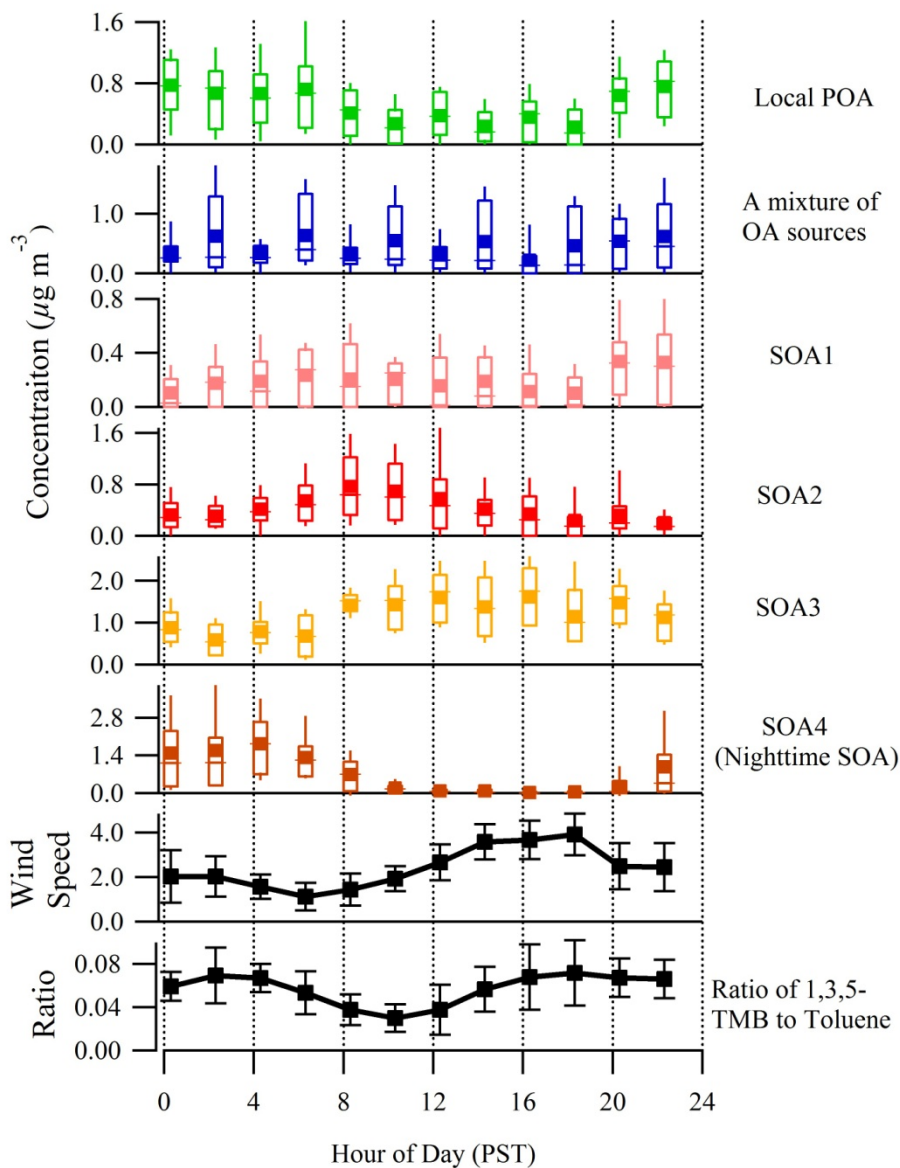
1294

1295 The best control strategy for each type of SOA (SOA1-4) to enable effective reductions
1296 in the regional OA concentration is likely different. The control of SOA precursor emissions on
1297 both local and regional scales are needed during the day, but control of regional SOA precursor
1298 emissions is likely to be most effective in reducing SOA in the afternoon when concentrations
1299 are currently highest. Reductions of gas-phase ammonia can also reduce the concentration of
1300 SOA2, but could also lead to the increase of the concentration of nighttime SOA. Further studies
1301 are needed to examine the effects of control of gas-phase ammonia on reductions of OA. At
1302 night, our observations suggest that biogenic SOA could contribute a significant fraction of total
1303 OA, yet its contribution is not well constrained.
1304



1306

1307 **Fig. 4.1** Organic compounds in each factor profile. Compounds are generally grouped into
 1308 hydrocarbons and oxygenated organic compounds.

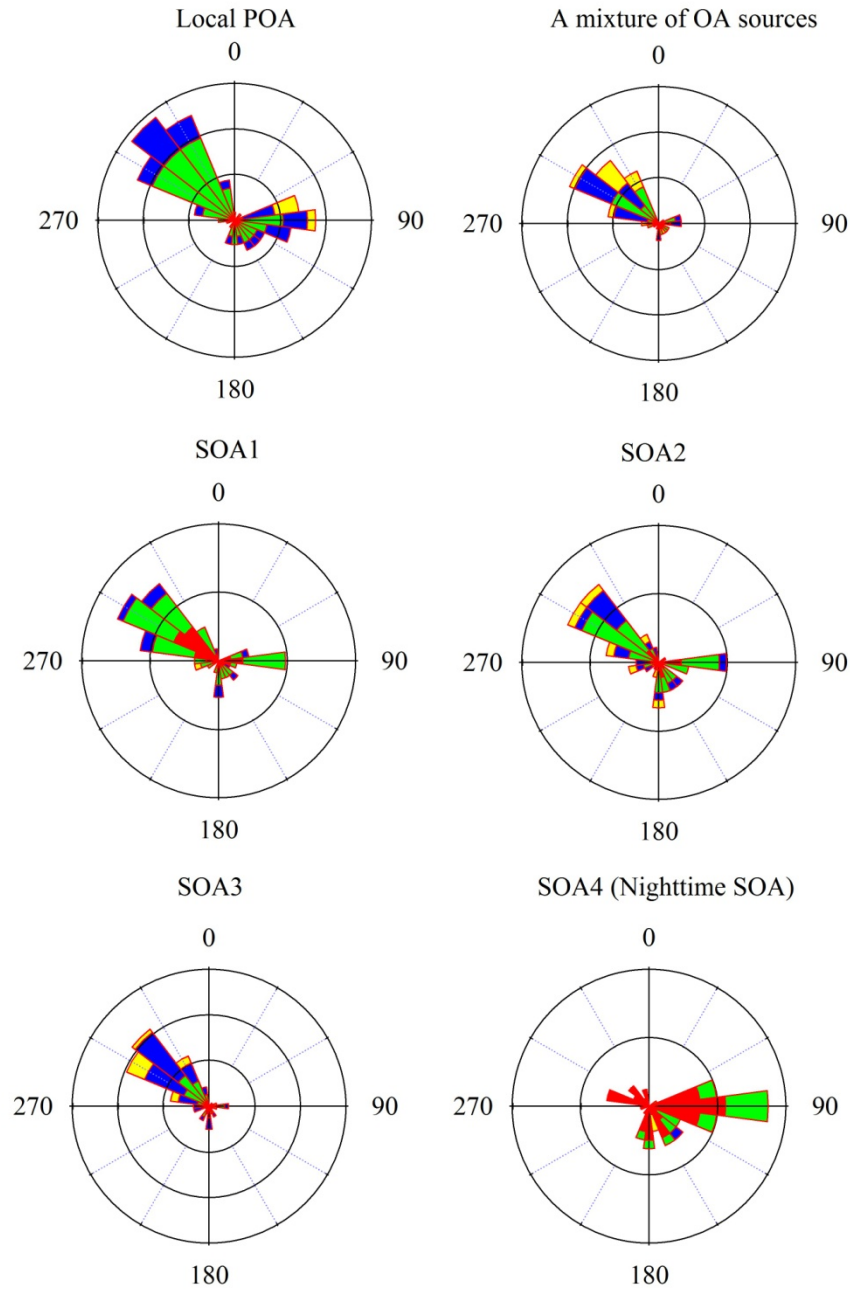


1309

1310

1311 **Fig. 4.2** Box plot of diurnal profile of the mass concentration of each factor and the average
 1312 diurnal profile of wind direction, and the ratio of 1,3,5-TMB to toluene. In the box plots, the
 1313 center line of each box is the median of the data, the top and bottom of the box are 75th and 25th
 1314 percentiles and top and bottom whiskers are 90th and 10th percentiles. The solid square maker is
 1315 the mean concentration. In average diurnal profiles, the mean value is plotted with \pm one
 1316 standard deviation.

1317



1318

1319

1320

1321

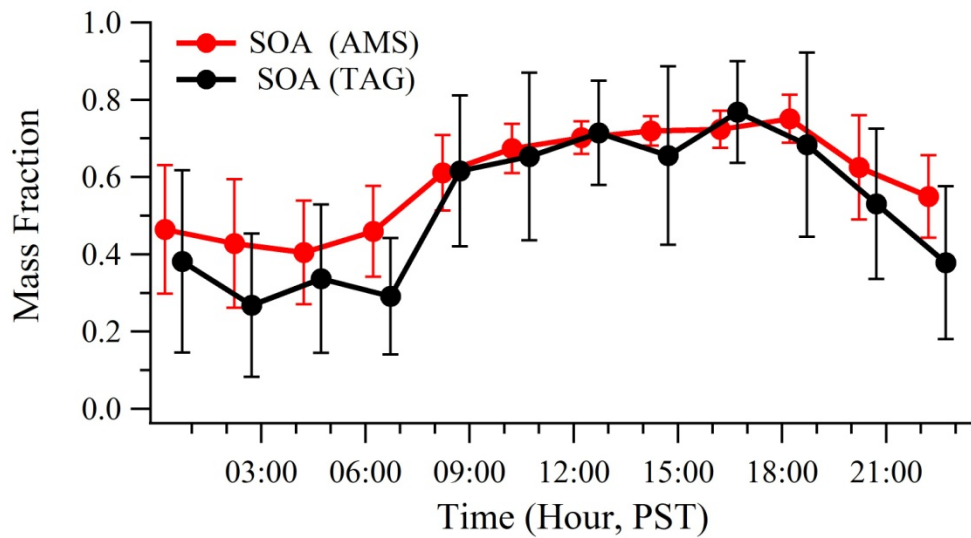
1322

1323

1324

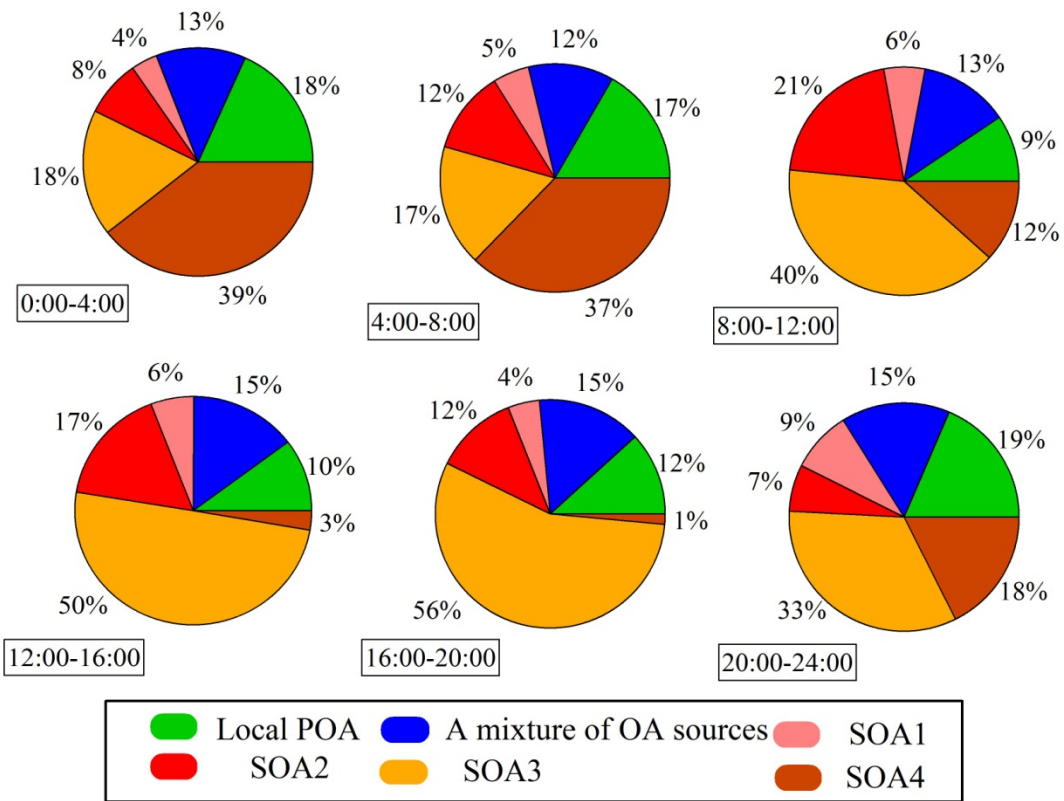
1325

Fig. 4.3 Wind rose plots for six PMF factors using only concentrations larger than the mean concentration in each factor to emphasize the major contributing source directions. The wind direction is shown in degrees with 0 (360) as north, 90 as east, 180 as south and 270 as west. The relative concentration level is indicated by different colors: yellow > blue > green > red. The frequency of observations is represented by the length of each wedge.



1326
 1327
 1328
 1329
 1330
 1331

Fig. 4.4 Average diurnal cycle of the mass fraction of OA identified as SOA by AMS PMF (Liu et al., 2012) and by TAG (this study). The TAG data are shift to the right for clarity.



1332
 1333
 1334
 1335
 1336

Fig. 4.5 Mean diurnal mass fraction contribution of each factor to total OA during six different times of day.

1337 **5.0 SUMMARY AND CONCLUSIONS**

1338 A TAG with improved separation of gases and particles through a denuder-based method
1339 was deployed in Bakersfield to measure organic species. As a result of this improvement, the
1340 TAG enables investigation of gas/particle partitioning of organic species and measurements of
1341 particle-phase organic species with minimal sampling artifacts caused by gas adsorption to the
1342 collection cell. The measurements were made during CalNex from May 31st to June 27th, 2010.
1343 The acquired data set consists of more than 100 compounds including alkanes, polycyclic
1344 aromatic hydrocarbons (PAHs), branched PAHs, acids, furanones, and other oxygenated
1345 compounds, which provided a large set of organic species for the investigation of SOA
1346 formation through a comparison between modeled and measured gas/particle partitioning and
1347 source apportionment of OA through positive matrix factorization (PMF) analysis.

1348

1349 **5.1 Gas-to-particle partitioning (SOA formation)**

1350 The gas/particle partitioning of phthalic acid, pinonaldehyde and 6, 10, 14-trimethyl-2-
1351 pentadecanone, three known oxidation products of hydrocarbons, was examined to explore the
1352 pathways of gas-to-particle partitioning of organic species whereby SOA was formed. Our
1353 results indicate that absorption into particles is the dominant pathway for 6, 10, 14-trimethyl-2-
1354 pentadecanone to contribute to SOA in the atmosphere. Absorption of gas-phase phthalic acid
1355 into particles can also contribute to observed particle-phase concentrations, but the major
1356 pathway to form particle-phase phthalic acid is likely through reactions with gas-phase ammonia
1357 to form condensable salts. The presence of pinonaldehyde in the particle phase when inorganic
1358 acids were neutralized suggests that strong acids are not required for the reactive uptake of
1359 pinonaldehyde into particles. The observed relationship between the cation-to-anion and the

1360 fraction of pinonaldehyde in the particles in our study did not display the effect of aerosol acidity
1361 on the reactive uptake of pinonaldehyde that has been previously reported for laboratory studies.
1362 The relationships between particle-phase pinonaldehyde and RH suggest that aerosol water
1363 content likely plays a significant role in the formation of particle-phase pinonaldehyde, although
1364 it is not the primary one.

1365

1366 **5.2 Major source contributions to OA**

1367 Six OA sources were identified including a POA source, a mixture of OA sources, and
1368 four types of SOA. Local vehicles are suggested to significantly contribute to POA. The four
1369 types of SOA (1-4) displayed distinct diurnal profiles. Three of the SOA factors (SOA1-3)
1370 displayed an enhancement in their contributions to OA at different times of the day. SOA1 and 2
1371 were mainly local while SOA3 was more regional. The fourth SOA factor mainly occurred
1372 during the night and showed contributions from both anthropogenic and biogenic SOA.

1373

1374 SOA was the dominant component of OA, with four distinct types of SOA accounting for
1375 a combined 72% of the total OA, varying diurnally from 66% at night to 78% during the day.
1376 The dominant type of OA varied throughout the day. Regional SOA (SOA3, 56%) was the
1377 largest contributor to the total OA during the afternoon and nighttime SOA (SOA4, 39%) was
1378 the largest contributor during the night. Local SOA (SOA2) contributed significantly in the
1379 morning, accounting for 21% of the total OA from 8:00 am to 12:00 pm PST. The smaller local
1380 SOA factor (SOA1) accounted for < 10% of total OA during all periods of the day.

1381

1382 The formation of SOA in this study occurred through multiple pathways. Direct gas-to-
1383 particle partitioning pathway is suggested to be the dominant formation pathway for SOA1 and
1384 3. Secondary gas-to-particle partitioning pathways played a major role in the formation of local
1385 SOA (SOA2). Particle-phase reactions also contributed to formation of nighttime SOA (SOA4),
1386 but their contributions are not well-constrained in this study.

1387

1388 **5.3 Implications for control of the OA concentration**

1389 In this study, speciated measurements of organic species in both gas and particle phases
1390 made with the TAG have not only provided particle-phase organics for PMF analysis to identify
1391 different OA sources, but also a unique dataset to examine the gas-to-particle partitioning
1392 pathways of SOA tracers. Our studies of OA sources and SOA formation pathways have
1393 provided insights into possibilities for effective control strategies to reduce the OA
1394 concentration.

1395

1396 In-situ measurements of both gas- and particle-phase organic compounds have clearly
1397 shown that multiple gas/particle partitioning pathways occur in the atmosphere and the SOA
1398 yields of oxygenated compounds through other gas/particle partitioning pathways are
1399 substantially higher relative to direct gas/particle partitioning. As a result, the control of
1400 emissions for species such as ammonia which are involved in the SOA formation should reduce
1401 SOA concentration. However, the efficiency of reductions of SOA concentrations by control of
1402 ammonia needs further investigation because the reduction of ammonia would increase the
1403 aerosol acidity and subsequently could increase the SOA formation through particle-phase
1404 reactions. Additionally, the occurrence and roles of different partitioning pathways can vary in

1405 different environments. Further in-situ, time-resolved measurements of gas/particle partitioning
1406 covering more oxygenated organic compounds are therefore suggested to identify the occurrence
1407 and examine the roles of SOA formation pathways in different areas with substantially different
1408 distributions of emission sources. We have examined the roles of multiple pathways in SOA
1409 formation in Bakersfield through inclusion of investigated SOA tracers into PMF analysis.

1410

1411 By performing PMF analysis on the particle-phase organic species, the contributions of
1412 six types of OA source factors to the OA mass were determined and SOA has been identified as
1413 the dominant OA component in Bakersfield, CA. SOA consists of four distinct SOA types,
1414 formed on both local and regional scales through different gas-to-particle partitioning pathways
1415 in this airshed. As a result, the best control strategy to reduce the OA concentration is to reduce
1416 emissions leading to the SOA formation, but the strategy for each type of SOA (SOA1-4) to
1417 enable effective reductions in the OA concentration is likely different. Control of SOA precursor
1418 emissions on both local and regional scales is needed to reduce the SOA concentration during the
1419 day, but control of regional precursor emissions is most effective to reduce SOA in the afternoon
1420 when the observed concentration was highest. Control of ammonia emissions should also reduce
1421 the concentration of local SOA (SOA2). However, as discussed above, control of ammonia
1422 emissions could also lead to more nighttime SOA. Further studies are needed to examine effects
1423 of the reduction of ammonia emissions on the reduction of the total OA. The contributions of
1424 both biogenic and anthropogenic precursors to the formation of nighttime SOA (SOA4) were
1425 evident, but neither of their contributions can be quantitatively determined in this study.
1426 Consequently, it remains unclear if the concentration of nighttime SOA could be effectively
1427 reduced by control of anthropogenic organic precursors.

1428 **6. Literature Cited**

- 1429
1430 Atkinson, R., and J. Arey (2003), Atmospheric degradation of volatile organic compounds, *Chem*
1431 *Rev*, *103*(12), 4605-4638.
1432
1433 Engelhart, G. J., L. Hildebrandt, E. Kostenidou, N. Mihalopoulos, N. M. Donahue, and S. N.
1434 Pandis (2011), Water content of aged aerosol, *Atmos Chem Phys*, *11*(3), 911-920.
1435
1436 Esteve, W., and B. Noziere (2005), Uptake and reaction kinetics of acetone, 2-butanone, 2,4-
1437 pentanedione, and acetaldehyde in sulfuric acid solutions, *J Phys Chem A*, *109*(48), 10920-
1438 10928.
1439
1440 Falkovich A. H. and Rudich Y. (2001) Analysis of semivolatile organic compounds in
1441 atmospheric aerosols by direct sample introduction thermal desorption GC/MS, *Environ. Sci.*
1442 *Technol.* *35*: 2326-2333.
1443
1444 Fine, P. M., Cass G. R., Simoneit, B. R. T. (2001) Chemical characterization of fine particle
1445 emissions from fireplace combustion of woods grown in the northeastern United States, *Environ.*
1446 *Sci. Technol.* *35*: 2665-2675.
1447
1448 Fine, P. M., B. Chakrabarti, M. Krudysz, J. J. Schauer, and C. Sioutas (2004), Diurnal variations
1449 of individual organic compound constituents of ultrafine and accumulation mode particulate
1450 matter in the Los Angeles basin, *Environ Sci Technol*, *38*(5), 1296-1304.
1451
1452 Fraser, M. P., G. R. Cass, B. R. T. Simoneit, and R. A. Rasmussen (1997), Air quality model
1453 evaluation data for organics .4. C-2-C-36 non-aromatic hydrocarbons, *Environ Sci Technol*,
1454 *31*(8), 2356-2367.
1455
1456 Gao, S., et al. (2004), Particle phase acidity and oligomer formation in secondary organic
1457 aerosol, *Environ Sci Technol*, *38*(24), 6582-6589.
1458
1459 Gentner, D.R., Isaacman, G., Worton, D.R., Chan, A.W.H., Dallmann, T.R., Davis, L., Liu, S.,
1460 Day, D.A., Russell, L.M., Wilson, K.R., Weber, R., Guha, A., Harley, R.A., and Goldstein, A.H.
1461 (2012), Secondary organic aerosol and the burning question of gas vs. diesel, Proceedings of the
1462 National Academy, submitted.
1463
1464 Goldstein, A. H., and I. E. Galbally (2007), Known and unexplored organic constituents in the
1465 earth's atmosphere, *Environ Sci Technol*, *41*(5), 1514-1521.
1466
1467 Goldstein, A.H., B.J. Williams, A. Miller, N.M. Kreisberg, and S.V. Hering, Hourly, In-Situ
1468 Quantitation of Organic Aerosol Marker Compounds, Final Report, California Air Resources
1469 Board Award No. 03-324, April 25, 2008.
1470

1471 Goldstein, A. H., C. D. Koven, C. L. Heald, and I. Y. Fung (2009), Biogenic carbon and
1472 anthropogenic pollutants combine to form a cooling haze over the southeastern United States, *P*
1473 *Natl Acad Sci USA*, 106(22), 8835-8840.
1474
1475 Goss, K. U., and R. P. Schwarzenbach (1998), Gas/solid and gas/liquid partitioning of organic
1476 compounds: Critical evaluation of the interpretation of equilibrium constants, *Environ Sci*
1477 *Technol*, 32(14), 2025-2032.
1478
1479 Greaves, R.C., Bakley, R.M., and Sievers, R.E. (1985), Rapid sampling and analysis of volatile
1480 constituents of airborne particulate matter, *Anal. Chem.*, 57: 2807-2815.
1481
1482 Hajek, M., J. Malek, and V. Bazant (1971), Kinetics of Thermal Decomposition of Ammonium
1483 Salts of Terephthalic and Isophthalic Acids, *Collect Czech Chem C*, 36(1), 84-&.
1484
1485 Heald, C. L., D. A. Ridley, S. M. Kreidenweis, and E. E. Drury (2010), Satellite observations cap
1486 the atmospheric organic aerosol budget, *Geophys Res Lett*, 37.
1487
1488 Heald, C. L., D. J. Jacob, R. J. Park, L. M. Russell, B. J. Huebert, J. H. Seinfeld, H. Liao, and R.
1489 J. Weber (2005), A large organic aerosol source in the free troposphere missing from current
1490 models, *Geophys Res Lett*, 32(18).
1491
1492 Helmig, D., and W. P. Harger (1994), Oh Radical-Initiated Gas-Phase Reaction-Products of
1493 Phenanthrene, *Sci Total Environ*, 148(1), 11-21.
1494
1495 Helmig, D., J. Arey, R. Atkinson, W. P. Harger, and P. A. Mcelroy (1992), Products of the Oh
1496 Radical-Initiated Gas-Phase Reaction of Fluorene in the Presence of Nox, *Atmos Environ a-Gen*,
1497 26(9), 1735-1745.
1498
1499 Hopke, P. K. (2003), Recent developments in receptor modeling, *J Chemometr*, 17(5), 255-265.
1500
1501 Hoyle, C. R., G. Myhre, T. K. Berntsen, and I. S. A. Isaksen (2009), Anthropogenic influence on
1502 SOA and the resulting radiative forcing, *Atmos Chem Phys*, 9(8), 2715-2728.
1503
1504 Iinuma, Y., O. Boge, Y. Miao, B. Sierau, T. Gnauk, and H. Herrmann (2005), Laboratory studies
1505 on secondary organic aerosol formation from terpenes, *Faraday Discuss*, 130, 279-294.
1506
1507 Jaeckels, J. M., M. S. Bae, and J. J. Schauer (2007), Positive matrix factorization (PMF) analysis
1508 of molecular marker measurements to quantify the sources of organic aerosols, *Environ Sci*
1509 *Technol*, 41(16), 5763-5769.
1510
1511 Jang, M. S., N. M. Czoschke, S. Lee, and R. M. Kamens (2002), Heterogeneous atmospheric
1512 aerosol production by acid-catalyzed particle-phase reactions, *Science*, 298(5594), 814-817.
1513
1514 Jimenez, J. L., et al. (2009), Evolution of Organic Aerosols in the Atmosphere, *Science*,
1515 326(5959), 1525-1529.
1516

1517 Kanakidou, M., et al. (2005), Organic aerosol and global climate modelling: a review, *Atmos*
1518 *Chem Phys*, 5, 1053-1123.
1519
1520 Khlystov, A., C. O. Stanier, S. Takahama, and S. N. Pandis (2005), Water content of ambient
1521 aerosol during the Pittsburgh air quality study, *J Geophys Res-Atmos*, 110(D7).
1522
1523 Kleindienst, T. E., M. Jaoui, M. Lewandowski, J. H. Offenberg, C. W. Lewis, P. V. Bhave, and
1524 E. O. Edney (2007), Estimates of the contributions of biogenic and anthropogenic hydrocarbons
1525 to secondary organic aerosol at a southeastern US location, *Atmos Environ*, 41(37), 8288-8300.
1526
1527 Kreisberg, N. M., S. V. Hering, B. J. Williams, D. R. Worton, and A. H. Goldstein (2009),
1528 Quantification of Hourly Speciated Organic Compounds in Atmospheric Aerosols, Measured by
1529 an In-Situ Thermal Desorption Aerosol Gas Chromatograph (TAG), *Aerosol Sci Tech*, 43(1), 38-
1530 52.
1531
1532 Kroll, J. H., and J. H. Seinfeld (2008), Chemistry of secondary organic aerosol: Formation and
1533 evolution of low-volatility organics in the atmosphere, *Atmos Environ*, 42(16), 3593-3624.
1534
1535 Kroll, J. H., N. L. Ng, S. M. Murphy, V. V, R. C. Flagan, and J. H. Seinfeld (2005), Chamber
1536 studies of secondary organic aerosol growth by reactive uptake of simple carbonyl compounds, *J*
1537 *Geophys Res-Atmos*, 110(D23).
1538
1539 Lewandowski, M., M. Jaoui, J. H. Offenberg, T. E. Kleindienst, E. O. Edney, R. J. Sheesley, and
1540 J. J. Schauer (2008), Primary and secondary contributions to ambient PM in the midwestern
1541 United States, *Environ Sci Technol*, 42(9), 3303-3309.
1542
1543 Li, Q. F., A. Wyatt, and R. M. Kamens (2009), Oxidant generation and toxicity enhancement of
1544 aged-diesel exhaust, *Atmos Environ*, 43(5), 1037-1042.
1545
1546 Liggio, J., and S. M. Li (2006), Reactive uptake of pinonaldehyde on acidic aerosols, *J Geophys*
1547 *Res-Atmos*, 111(D24).
1548
1549 Liu et al. (2012), Secondary organic aerosol formation from fossil fuel sources contribute
1550 majority of summertime organic mass at Bakersfield, Geophysical Research-atmosphere, In
1551 press.
1552
1553 Magliano, K. L., V. M. Hughes, L. R. Chinkin, D. L. Coe, T. L. Haste, N. Kumar, and F. W.
1554 Lurmann (1999), Spatial and temporal variations in PM10 and PM2.5 source contributions and
1555 comparison to emissions during the 1995 integrated monitoring study, *Atmos Environ*, 33(29),
1556 4757-4773.
1557
1558 Markovic, M. Z.; VandenBoer, T. C.; Murphy, J. G. Characterization and optimization of an
1559 online system for the simultaneous measurement of atmospheric water-soluble constituents in the
1560 gas and particle phases. *J. Environ. Monitor.* **2012**, 14, 1872-1884

1561 Na, K., C. Song, C. Switzer, and D. R. Cocker (2007), Effect of ammonia on secondary organic
1562 aerosol formation from alpha-Pinene ozonolysis in dry and humid conditions, *Environ Sci*
1563 *Technol*, 41(17), 6096-6102.
1564
1565 Neusüss, C., Pelzing, M., Plewka, A., and Herrmann, H. (2000), A new analytical approach for
1566 size-resolved speciation of organic compounds in atmospheric aerosol particles: Methods and
1567 first results, *J. Geophysical Research* 105, 4513-4527.
1568
1569 Nguyen, T. B., P. J. Roach, J. Laskin, A. Laskin, and S. A. Nizkorodov (2011), Effect of
1570 humidity on the composition of isoprene photooxidation secondary organic aerosol, *Atmos Chem*
1571 *Phys*, 11(14), 6931-6944.
1572
1573 Nolte C. G., Schauer J. J., Cass, G. R., and Simoneit, B. R. T. (1999), Highly polar organic
1574 compounds present in meat smoke, *Environ. Sci. Technol.*, 33: 3313-3316.
1575
1576 Odum, J. R., T. P. W. Jungkamp, R. J. Griffin, R. C. Flagan, and J. H. Seinfeld (1997), The
1577 atmospheric aerosol-forming potential of whole gasoline vapor, *Science*, 276(5309), 96-99.
1578
1579 Paatero, P., and U. Tapper (1993), Analysis of Different Modes of Factor-Analysis as Least-
1580 Squares Fit Problems, *Chemometr Intell Lab*, 18(2), 183-194.
1581
1582 Pankow, J. F. (1994), An Absorption-Model of Gas-Particle Partitioning of Organic-Compounds
1583 in the Atmosphere, *Atmos Environ*, 28(2), 185-188.
1584
1585 Reff, A., S. I. Eberly, and P. V. Bhave (2007), Receptor modeling of ambient particulate matter
1586 data using positive matrix factorization: Review of existing methods, *J Air Waste Manage*, 57(2),
1587 146-154.
1588
1589 Robinson, A. L., R. Subramanian, N. M. Donahue, A. Bernardo-Bricker, and W. F. Rogge
1590 (2006), Source apportionment of molecular markers and organic aerosol. 3. Food cooking
1591 emissions, *Environ Sci Technol*, 40(24), 7820-7827.
1592
1593 Robinson, A. L., N. M. Donahue, M. K. Shrivastava, E. A. Weitkamp, A. M. Sage, A. P.
1594 Grieshop, T. E. Lane, J. R. Pierce, and S. N. Pandis (2007), Rethinking organic aerosols:
1595 Semivolatile emissions and photochemical aging, *Science*, 315(5816), 1259-1262.
1596
1597 Rogge, W. F., Hildemann, L. M. Mazurek, M. A., Cass, G. R., and Simoneit, B. R. T. (1997a),
1598 Sources of fine organic aerosol. 7. hot asphalt roofing tar pot fumes, *Environ. Sci. Technol.*, 31,
1599 2726-2730.
1600
1601 Rogge, W. F., Hildemann, L. M. Mazurek, M. A., Cass, G. R., and Simoneit, B. R. T. (1997b),
1602 Sources of fine organic aerosol. 8. boilers burning no. 2 distillate fuel oil, *Environ. Sci. Technol.*,
1603 31, 2731-2737.
1604

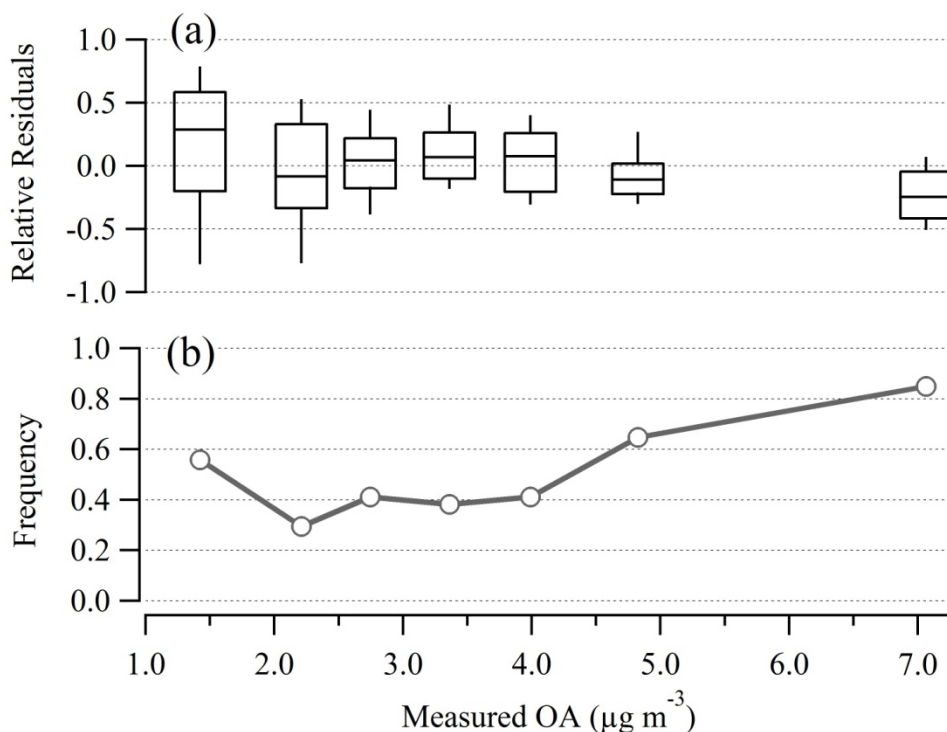
1605 Rogge, W. F., Hildemann, L. M. Mazurek, M. A. and Cass, G. R. (1998), Sources of fine organic
1606 aerosol 9: pine oak and synthetic log combustion in residential fireplaces, *Environ Sci Technol.*
1607 32, 13-22.
1608
1609 Russell, L. M.; Bahadur, R.; Hawkins, L. N.; Allan, J.; Baumgardner, D.; Quinn, P. K.; Bates, T.
1610 S. (2009) Organic aerosol characterization by complementary measurements of chemical bonds
1611 and molecular fragments. *Atmos. Environ.*, 43, 6100-6105.
1612
1613 Schauer, J. J., and G. R. Cass (2000), Source apportionment of wintertime gas-phase and
1614 particle-phase air pollutants using organic compounds as tracers, *Environ Sci Technol*, 34(9),
1615 1821-1832.
1616
1617 Schauer, J. J., M. J. Kleeman, G. R. Cass, and B. R. T. Simoneit (1999a), Measurement of
1618 emissions from air pollution sources. 1. C-1 through C-29 organic compounds from meat
1619 charbroiling, *Environ Sci Technol*, 33(10), 1566-1577.
1620
1621 Schauer, J. J., M. J. Kleeman, G. R. Cass, and B. R. T. Simoneit (1999b), Measurement of
1622 emissions from air pollution sources. 2. C-1 through C-30 organic compounds from medium
1623 duty diesel trucks, *Environ Sci Technol*, 33(10), 1578-1587.
1624
1625 Schauer, J. J., M. P. Fraser, G. R. Cass, and B. R. T. Simoneit (2002a), Source reconciliation of
1626 atmospheric gas-phase and particle-phase pollutants during a severe photochemical smog
1627 episode, *Environ Sci Technol*, 36(17), 3806-3814.
1628
1629 Schauer, J. J., M. J. Kleeman, G. R. Cass, and B. R. T. Simoneit (2002b), Measurement of
1630 emissions from air pollution sources. 5. C-1-C-32 organic compounds from gasoline-powered
1631 motor vehicles, *Environ Sci Technol*, 36(6), 1169-1180.
1632
1633 Schauer, J. J., W. F. Rogge, L. M. Hildemann, M. A. Mazurek, G. R. Cass, and B. R. T. Simoneit
1634 (1996), Source apportionment of airborne particulate matter using organic compounds as tracers,
1635 *Atmos Environ*, 30(22), 3837-3855.
1636
1637 Schuster, G. L., B. Lin, and O. Dubovik (2009), Remote sensing of aerosol water uptake,
1638 *Geophys Res Lett*, 36.
1639
1640 Seinfeld, J. H., and J. F. Pankow (2003), Organic atmospheric particulate material, *Annu Rev*
1641 *Phys Chem*, 54, 121-140.
1642
1643 Shrivastava, M. K., R. Subramanian, W. F. Rogge, and A. L. Robinson (2007), Sources of
1644 organic aerosol: Positive matrix factorization of molecular marker data and comparison of results
1645 from different source apportionment models, *Atmos Environ*, 41(40), 9353-9369.
1646
1647 Spracklen, D. V., et al. (2011), Aerosol mass spectrometer constraint on the global secondary
1648 organic aerosol budget, *Atmos Chem Phys*, 11(23), 12109-12136.
1649

1650 Stone, E. A., J. B. Zhou, D. C. Snyder, A. P. Rutter, M. Mieritz, and J. J. Schauer (2009), A
1651 Comparison of Summertime Secondary Organic Aerosol Source Contributions at Contrasting
1652 Urban Locations, *Environ Sci Technol*, 43(10), 3448-3454.
1653
1654 Strader, R., F. Lurmann, and S. N. Pandis (1999), Evaluation of secondary organic aerosol
1655 formation in winter, *Atmos Environ*, 33(29), 4849-4863.
1656
1657 Subramanian, R., N. M. Donahue, A. Bernardo-Bricker, W. F. Rogge, and A. L. Robinson
1658 (2007), Insights into the primary-secondary and regional-local contributions to organic aerosol
1659 and PM_{2.5} mass in Pittsburgh, Pennsylvania, *Atmos Environ*, 41(35), 7414-7433.
1660
1661 Tillmann, R., M. Hallquist, A. M. Jonsson, A. Kiendler-Scharr, H. Saathoff, Y. Iinuma, and T. F.
1662 Mentel (2010), Influence of relative humidity and temperature on the production of
1663 pinonaldehyde and OH radicals from the ozonolysis of alpha-pinene, *Atmos Chem Phys*, 10(15),
1664 7057-7072.
1665
1666 Tolocka, M. P., M. Jang, J. M. Ginter, F. J. Cox, R. M. Kamens, and M. V. Johnston (2004),
1667 Formation of oligomers in secondary organic aerosol, *Environ Sci Technol*, 38(5), 1428-1434.
1668
1669 Turpin, B. J., P. Saxena, and E. Andrews (2000), Measuring and simulating particulate organics
1670 in the atmosphere: problems and prospects, *Atmos Environ*, 34(18), 2983-3013.
1671
1672 Turpin, B. J., J. J. Huntzicker, S. M. Larson, and G. R. Cass (1991), Los-Angeles Summer
1673 Midday Particulate Carbon - Primary and Secondary Aerosol, *Environ Sci Technol*, 25(10),
1674 1788-1793.
1675
1676 Ulbrich, I. M., M. R. Canagaratna, Q. Zhang, D. R. Worsnop, and J. L. Jimenez (2009),
1677 Interpretation of organic components from Positive Matrix Factorization of aerosol mass
1678 spectrometric data, *Atmos Chem Phys*, 9(9), 2891-2918.
1679
1680 Volkamer, R., J. L. Jimenez, F. San Martini, K. Dzepina, Q. Zhang, D. Salcedo, L. T. Molina, D.
1681 R. Worsnop, and M. J. Molina (2006), Secondary organic aerosol formation from anthropogenic
1682 air pollution: Rapid and higher than expected, *Geophys Res Lett*, 33(17).
1683
1684 Waterman, D., Horsfield, B., Leistner, F., Hall, K., and Smith, S. (2000), Quantification of
1685 Polycyclic Aromatic Hydrocarbons in the NIST Standard Reference Material (SRM1649A)
1686 Urban Dust Using Thermal Desorption GC/MS, *Analytical Chemistry*, 2000; 72(15); 3563-3567.
1687
1688 Williams, B.J.; Goldstein, A.H.; Millet, D.B.; Holzinger, R; Kreisberg, N.M.; Hering, S.V.; White, A.B.;
1689 Worsnop, D.R.; Allan, J.D.; Jimenez, J.L., (2007), Chemical speciation of organic aerosol during the
1690 International Consortium for Atmospheric Research on Transport and Transformation 2004: Results from
1691 in situ measurements *Journal of Geophysical Research*, 112: D10, #D10S26.
1692
1693 Williams, B. J., A. H. Goldstein, N. M. Kreisberg, and S. V. Hering (2006), An in-situ
1694 instrument for speciated organic composition of atmospheric aerosols: Thermal Desorption
1695 Aerosol GC/MS-FID (TAG), *Aerosol Sci Tech*, 40(8), 627-638.
1696

1697 Williams, B. J., A. H. Goldstein, N. M. Kreisberg, S. V. Hering, D. R. Worsnop, I. M. Ulbrich,
1698 K. S. Docherty, and J. L. Jimenez (2010a), Major components of atmospheric organic aerosol in
1699 southern California as determined by hourly measurements of source marker compounds, *Atmos*
1700 *Chem Phys*, *10*(23), 11577-11603.
1701
1702 Williams, B. J., A. H. Goldstein, N. M. Kreisberg, and S. V. Hering (2010b), In situ
1703 measurements of gas/particle-phase transitions for atmospheric semivolatile organic compounds,
1704 *P Natl Acad Sci USA*, *107*(15), 6676-6681.
1705
1706 Worton, D. R., et al. (2011), Origins and composition of fine atmospheric carbonaceous aerosol
1707 in the Sierra Nevada Mountains, California, *Atmos Chem Phys*, *11*(19), 10219-10241.
1708
1709 Xue, J.; Lau, A. K. H.; Yu, J. Z. (2011) A study of acidity on PM_{2.5} in Hong Kong using online
1710 ionic chemical composition measurements. *Atmos. Environ.*, *45*, 7081-7088.
1711
1712
1713 Zhang, Q., J. L. Jimenez, D. R. Worsnop, and M. Canagaratna (2007a), A case study of urban
1714 particle acidity and its influence on secondary organic aerosol, *Environ Sci Technol*, *41*(9), 3213-
1715 3219.
1716
1717 Zhang, Q., J. L. Jimenez, M. R. Canagaratna, I. M. Ulbrich, N. L. Ng, D. R. Worsnop, and Y. L.
1718 Sun (2011), Understanding atmospheric organic aerosols via factor analysis of aerosol mass
1719 spectrometry: a review, *Anal Bioanal Chem*, *401*(10), 3045-3067.
1720
1721 Zhang, Q., et al. (2007b), Ubiquity and dominance of oxygenated species in organic aerosols in
1722 anthropogenically-influenced Northern Hemisphere midlatitudes, *Geophys Res Lett*, *34*(13).
1723
1724 Zhang, Y., R. J. Sheesley, J. J. Schauer, M. Lewandowski, M. Jaoui, J. H. Offenberg, T. E.
1725 Kleindienst, and E. O. Edney (2009), Source apportionment of primary and secondary organic
1726 aerosols using positive matrix factorization (PMF) of molecular markers, *Atmos Environ*, *43*(34),
1727 5567-5574.
1728
1729 Zhao, Y., N.K., Kreisberg, D.R., Worton, G., Isaacman, R.J., Weber, M. Z., Markovic, T.C.,
1730 Vandenboer, S., Liu, D.A., Douglas, J.G., Murphy, L.M., Russell, S.V., Hering, A.H., Goldstein,
1731 (2012), Insights for SOA formation mechanisms from measured gas/particle partitioning of
1732 specific organic tracer compounds. Submitted to *Environ Sci Technol*
1733
1734 Zheng, M., G. R. Cass, J. J. Schauer, and E. S. Edgerton (2002), Source apportionment of PM_{2.5}
1735 in the southeastern United States using solvent-extractable organic compounds as tracers,
1736 *Environ Sci Technol*, *36*(11), 2361-2371.
1737
1738

1739
1740
1741

Appendix A An Supplemental Figure for Chapter 4



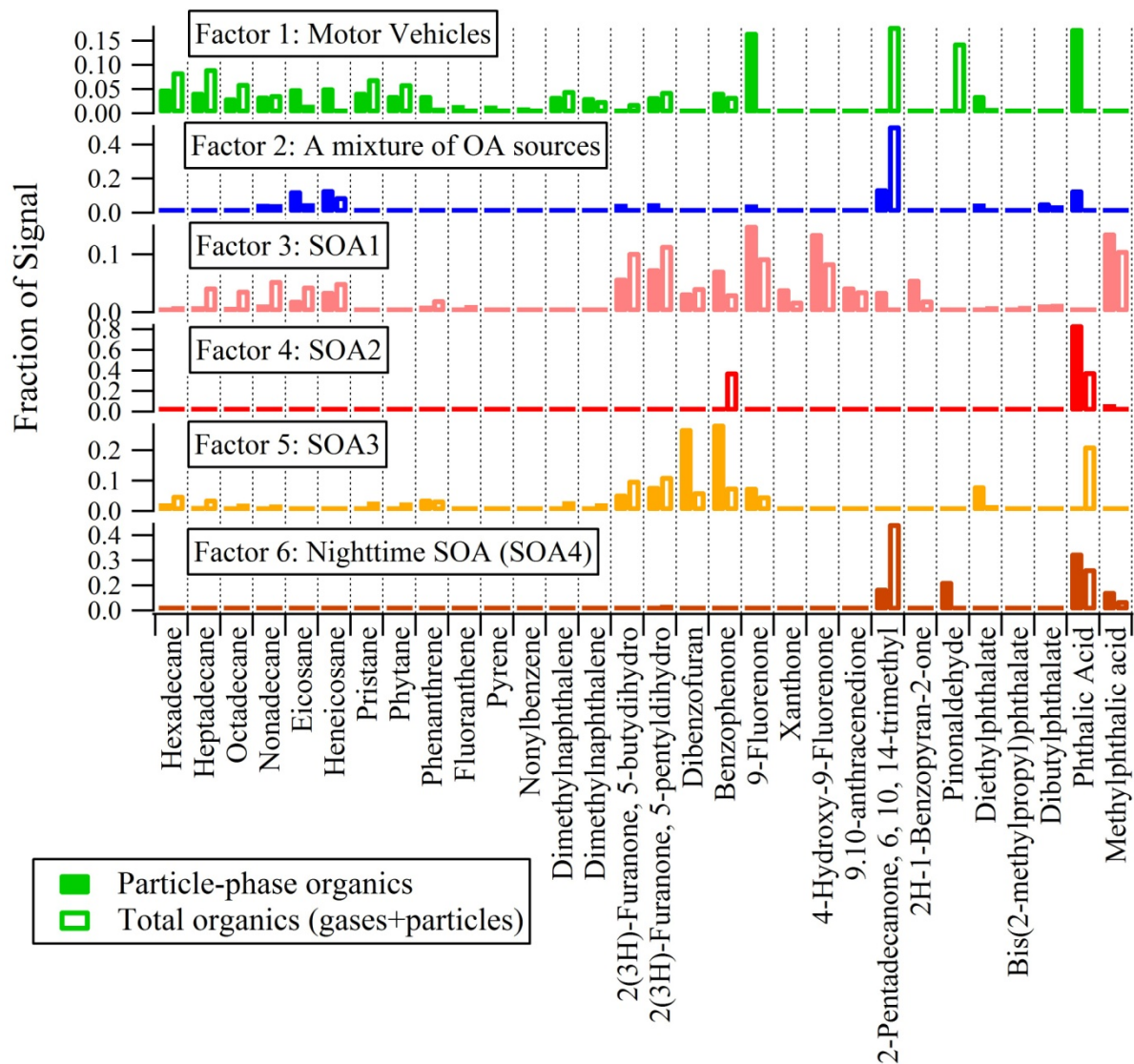
1742
1743 **Fig. A1** (a) The box plot of the relative residues determined using the difference between
1744 reconstructed and measured OA divided by measured OA. The center line of each box is the
1745 median of the data, the top and bottom of the box are 75th and 25th percentiles and top and
1746 bottom whiskers are 90th and 10th percentiles. The data points are evenly distributed to each
1747 interval. (b) the frequency of the different atmospheric OA concentrations occurred at night.

1748 **Appedix B**

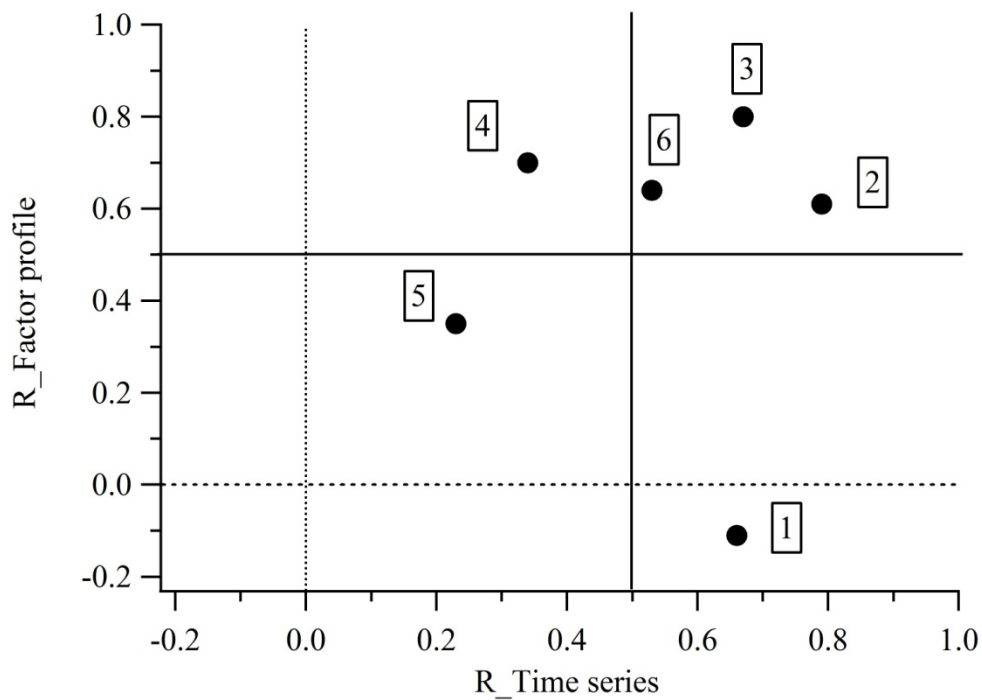
1749 **Effect of including gas-phase contributions to particle-phase SVOCs on the PMF solution**

1750 Many compounds are present in the particle phase, especially SOA tracers are SVOCs. As a
1751 result of the utility of SVOCs in PMF analysis, inclusion of gas-phase contributions can bias the
1752 temporal variability in particle-phase concentrations of these SVOCs and subsequently lead to
1753 changes in correlations between different compounds, which PMF analysis relies on to extract
1754 different factors and explain the OA observations. The effect of gas-phase contributions on the
1755 PMF solution, caused by gas-phase organic adsorption to the collection cell when sampling in
1756 bypass mode (no denuder), is shown by comparison of the same number of factors extracted
1757 from the same group of compounds with or without gas-phase contributions. The factor profiles
1758 from measurements of organics with and without gas-phase contributions are significantly
1759 different (Fig S2). To visualize the difference caused by gas-phase contributions, the correlation
1760 between two factor profiles and the correlation between their time series were plotted against
1761 each other. As shown in Fig. S3, the difference in the temporal variability and chemical
1762 composition of the factors are apparent for factor 1, 4, 5. Although the correlation coefficients (r)
1763 for both temporal variability and chemical composition of the factor 2, 3, 6 are good, they are
1764 still less than 0.8. This comparison establishes that the exclusion of gas-phase contributions to
1765 SVOCs used in PMF analysis is crucial to achieve a correct source apportionment.

1766



1767
 1768 **Fig. B1** Factor profiles of factors extracted by PMF analysis from the same compound list with
 1769 and without inclusion of gas-phase contributions to the measured SVOCs.
 1770



1771

1772 **Fig. B2** Correlation of the timeline of observations and correlation of factor profile of the
 1773 corresponding factor extracted by PMF analysis from the dataset with or without inclusion of
 1774 gas-phase contributions. The labeled number refers to the factor number in Figure B1.

1775

1776

1777

1778

1779

1780

1781

1782

1783

1784

1785

1786

1787

1788

1789

Appendix C

1790

1791

1792 Liu, S., L. Ahlm, D.A. Day, L.M. Russell, Y. Zhao, D.R. Gentner, R.J. Weber, A.H. Goldstein,
1793 M. Jaoui, J.H. Offenberg, T.E. Kleindienst, C. Rubitschun, J.D. Surratt, R.J. Sheesley, and S.
1794 Scheller, Secondary organic aerosol formation from fossil fuel sources contribute majority of
1795 summertime organic mass at Bakersfield, *J. Geophys. Res.*, 117, D00V26,
1796 doi:10.1029/2012JD018170, 2012.

1797

1798 **Abstract**

1799 Secondary organic aerosols (SOA), known to form in the atmosphere from oxidation of volatile
1800 organic compounds (VOCs) emitted by anthropogenic and biogenic sources, are a poorly
1801 understood but substantial component of atmospheric particles. In this study, we examined the
1802 chemical and physical properties of SOA at Bakersfield, California, a site influenced by
1803 anthropogenic and terrestrial biogenic emissions. Factor analysis was applied to the infrared and
1804 mass spectra of fine particles to identify sources and atmospheric processing that contributed to
1805 the organic mass (OM). We found that OM accounted for 56% of submicron particle mass, with
1806 SOA components contributing 80% to 90% of OM from 15 May to 29 June 2010. SOA formed
1807 from alkane and aromatic compounds, the two major classes of vehicle-emitted hydrocarbons,
1808 accounted for 65%OM(72% SOA). The alkane and aromatic SOA components were associated
1809 with 200 nm to 500 nm accumulation mode particles, likely from condensation of daytime
1810 photochemical products of VOCs. In contrast, biogenic SOA likely formed from condensation of
1811 secondary organic vapors, produced from NO₃ radical oxidation reactions during nighttime
1812 hours, on 400 nm to 700 nm sized primary particles, and accounted for less than 10% OM. Local
1813 petroleum operation emissions contributed 13% to the OM, and the moderate O/C (0.2) of this
1814 factor suggested it was largely of secondary origin. Approximately 10% of organic aerosols in
1815 submicron particles were identified as either vegetative detritus (10%) or cooking activities
1816 (7%), from Fourier transform infrared spectroscopic and aerosol mass spectrometry
1817 measurements, respectively. While the mass spectra of several linearly independent SOA
1818 components were nearly identical and external source markers were needed to separate them,
1819 each component had distinct infrared spectrum, likely associated with the source-specific VOCs
1820 from which they formed.

Appendix D

1821
1822
1823
1824
1825
1826
1827
1828
1829
1830
1831
1832
1833
1834
1835
1836
1837
1838
1839
1840
1841
1842
1843
1844
1845
1846
1847
1848
1849
1850

O'Brien, R.E., A. Laskin, J. Laskin, S. Liu, R. Weber, L.M. Russell, A.H. Goldstein, Molecular Characterization of Organic Aerosol Using Nanospray Desorption/Electrospray Ionization Mass Spectrometry: CalNex 2010 field study, *Atmospheric Environment*, DOE: 10.1016/j.atmosenv.2012.11.056, Available online 6 December 2012.

Abstract

Aerosol samples from the CalNex 2010 field study were analyzed using high resolution mass spectrometry (HR-MS) coupled to a nanospray-desorption/electrospray ionization (nano-DESI) source. The samples were collected in Bakersfield, CA on June 22-23, 2010. The chemical formulas of over 850 unique molecular species were detected in the mass range of 50-400 m/z using positive mode ESI of aerosol samples in the 0.18-0.32 μm size range. Our analysis focused on identification of two main groups: compounds containing only carbon, hydrogen, and oxygen (CHO), and nitrogen-containing organic compounds (NOC). The NOC accounted for 40% (by number) of the compounds observed in the afternoon, and for 52% in the early morning samples. By comparing plausible reactant-product pairs, we propose that over 50% of the NOC in each sample could have been formed through reactions transforming carbonyls into imines. The CHO only compounds were dominant in the afternoon suggesting a photochemical source. The average O/C ratios of all observed compounds were fairly consistent throughout the day, ranging from 0.33 in the morning to 0.37 at night. We conclude that both photooxidation and ammonia chemistry may play a role in forming the compounds observed in this mixed urban-rural environment.

Appendix E

1851
1852
1853
1854
1855
1856
1857
1858
1859
1860
1861
1862
1863
1864
1865
1866
1867
1868
1869
1870
1871
1872
1873
1874
1875
1876
1877
1878
1879
1880

O'Brien, R., T. Nguyen, A. Laskin, J. Laskin, P. Hayes, S. Liu, J.-L. Jimenez, L. Russell, A.H. Goldstein, Probing Molecular Associations of Field-Collected and Laboratory-Generated SOA with Nano-DESI High-Resolution Mass Spectrometry, *J. Geophys. Res.*, CalNex Special Issue, In Press.

Abstract

Aerosol samples from the 2010 CalNex field study in Bakersfield (BF) and Pasadena, Los Angeles (LA) were analyzed using positive mode nanospray-desorption electrospray ionization mass spectrometry (nano-DESI-MS). Secondary organic aerosol (SOA) produced in a photochemical chamber by photooxidation of diesel (DSL) fuel and isoprene (ISO) under humid, high-NO_x conditions, was analyzed for comparison. Three groups of organic compounds with zero, one, or two nitrogen atoms in their molecular formulas (0N, 1N, 2N) were compared in detail. The composition of ambient SOA exhibited greater overlap with DSL than with ISO. The overlap of the chamber experiments with the BF data was relatively consistent throughout the day while the overlap with LA data increased significantly in the noon-6pm sample, consistent with the SOA plume arriving from downtown Los Angeles. BF samples were more oxidized, contained more organic nitrogen, and had more overlap with the chamber data compared to LA samples. The addition of gaseous ammonia (NH₃) to the DSL experiment was necessary to generate many of the 2N compounds observed in BF. This analysis demonstrates that DSL and ISO were important sources but cannot account for all of the observed ambient compounds indicating that other sources of organics were also likely important.

Appendix F: Data Sets Description

1881
1882
1883 Data set **TAG_DATA_20100531_RA**
1884
1885 General:
1886 This data set contains ambient concentrations of organic compounds measured with TAG during
1887 the CalNex 2010 campaign in Bakersfield. The concentration units are ng per cubic meter.
1888
1889 Data items filled with the value -9999 denote “lower than detection limit”
1890
1891 Column descriptions (numbering refers to column number):
1892 0. “TAG_mid_pst” sampling midpoint in seconds since May 31st. Note that all times
1893 are local standard time (Pacific Standard Time = PST)
1894 1. “TAG_Start_pst” sampling start point in seconds since May 31st
1895 2. “TAG_stop_pst” sampling end point in seconds since May 31st
1896 3. “TAG_DOY” Day of the year
1897 4. “Runtype” Indicates which inlet was used: 1 = denuded samples (only
1898 particle-phase organics); 2 = undenuded samples (gas and particle
1899 phase organics)
1900 5. “CNC1” n-tridecane
1901 6. “CNC2” n-tetradecane
1902 7. “CNC3” n-pentadecane
1903 8. “CNC4” n-hexadecane
1904 9. “CNC5” n-heptadecane
1905 10. “CNC6” n-octadecane
1906 11. “CNC7” n-nonadecane
1907 12. “CNC8” n-eicosane
1908 13. “CNC9” n-heneicosane
1909 14. “CNC10” n-docosane
1910 15. “CNC11” n-tricosane
1911 16. “CNC12” n-tetracosane
1912 17. “CNC13” n-pentacosane
1913 18. “CNC14” n-hexacosane
1914 19. “CNC15” n-heptacosane

1915	20. "CNC16"	n-octacosane
1916	21. "CNC17"	n-nonacosane
1917	22. "CNC18"	n-triacontane
1918	23. "CNC19"	n-hentriacontane
1919	24. "CNC20"	Pristane
1920	25. "CNC21"	Phytane
1921	26. "CNC22"	Acenaphthylene
1922	27. "CNC23"	Fluorene
1923	28. "CNC24"	Phenanthrene
1924	29. "CNC25"	Anthracene
1925	30. "CNC26"	Fluoranthene
1926	31. "CNC27"	Pyrene
1927	32. "CNC28"	1,2-Benzanthracene
1928	33. "CNC29"	Chrysene
1929	34. "CNC30"	Benzo(b)fluoranthene
1930	35. "CNC31"	Benzo(k)fluoranthene
1931	36. "CNC32"	Benzo(a)fluoranthene
1932	37. "CNC33"	Methylnaphthalene
1933	38. "CNC34"	Ethtylnaphthalene
1934	39. "CNC35"	Dimethylnaphthalene
1935	40. "CNC36"	Dimethylnaphthalene
1936	41. "CNC37"	Dimethylnaphthalene
1937	42. "CNC38"	Trimethylnaphthalene
1938	43. "CNC39"	Trimethylnaphthalene
1939	44. "CNC40"	Naphthalene, 2-phenyl
1940	45. "CNC41"	Methylphenanthracene
1941	46. "CNC42"	Methylphenanthracene
1942	47. "CNC43"	Methylanthracene
1943	48. "CNC44"	Methylanthracene
1944	49. "CNC45"	Phenanthrene, 1-methyl-7-(1-methylethyl)-
1945	50. "CNC46"	MethylPyrene
1946	51. "CNC47"	MethylPyrene
1947	52. "CNC48"	m-Terphenyl, 5-phenyl-

1948	53. "CNC49"	2(3H)-Furanone, 5-butyldihydro
1949	54. "CNC50"	2(3H)-Furanone, 5-pentyldihydro
1950	55. "CNC51"	2(3H)-Furanone, 5-hexyldihydro
1951	56. "CNC52"	2(3H)-Furanone, 5-heptyldihydro
1952	57. "CNC53"	2(3H)-Furanone, 5-octyldihydro
1953	58. "CNC54"	2(3H)-Furanone, 5-nonyldihydro
1954	59. "CNC55"	2(3H)-Furanone, 5-decyldihydro
1955	60. "CNC56"	Dibenzofuran
1956	61. "CNC57"	Benzophenone
1957	62. "CNC58"	9-Fluorenone
1958	63. "CNC59"	Xanthone
1959	64. "CNC60"	4-Hydroxy-9-fluorenone
1960	65. "CNC61"	9, 10-Anthracenedione
1961	66. "CNC62"	Nonanoic acid
1962	67. "CNC63"	Decanoic acid
1963	68. "CNC64"	Dodecanoic acid
1964	69. "CNC65"	Tetradecanoic acid
1965	70. "CNC66"	Hexadecanoic acid
1966	71. "CNC67"	$\alpha\beta$ 20R-cholestane
1967	72. "CNC68"	$\alpha\alpha$ -20R-cholestane
1968	73. "CNC69"	$\alpha\beta\beta$ 20R 24S-methylcholestane
1969	74. "CNC70"	$\alpha\alpha\alpha$ 20R 24R-ethylcholestane
1970	75. "CNC71"	$\alpha\beta\beta$ 20R 24R-ethylcholestane
1971	76. "CNC72"	17 α (H)-22,29,30-trisnorhopane
1972	77. "CNC73"	17 α (H),21 β (H)-30-norhopane
1973	78. "CNC74"	17 α (H),21 β (H)-hopane
1974	79. "CNC75"	17 α (H),21 β (H)-22R-homohopane
1975	80. "CNC76"	17 α (H),21 β (H)- 22S-homohopane
1976	81. "CNC77"	undecylcyclohexane
1977	82. "CNC78"	dodecylcyclohexane
1978	83. "CNC79"	Tridecylcyclohexane
1979	84. "CNC80"	Tetradecylcyclohexane
1980	85. "CNC81"	Pentadecylcyclohexane

1981	86. "CNC82"	Hexadecylclohexane
1982	87. "CNC83"	Heptadecylclohexane
1983	88. "CNC84"	Octadecylclohexane
1984	89. "CNC85"	Nonadecylclohexane
1985	90. "CNC86"	Eicosylclohexane
1986	91. "CNC87"	1,2-Benedicarboxylic acid, diethyl ester
1987	92. "CNC88"	1,2-Benedicarboxylic acid, Bis(2-methylpropyl) ester
1988	93. "CNC89"	1,2-Benedicarboxylic acid, dibutyl ester
1989	94. "CNC90"	1,2-Benedicarboxylic acid, butyl phenylmethyl ester
1990	95. "CNC91"	1,2-Benedicarboxylic acid, Bis(2-ethylhexyl) ester
1991	96. "CNC92"	Undecanone
1992	97. "CNC93"	Dodecanone
1993	98. "CNC94"	Tridecanone
1994	99. "CNC95"	Tetradecanone
1995	100. "CNC96"	Pentadecanone
1996	101. "CNC97"	Hexadecanone
1997	102. "CNC98"	2-Pentadecanone, 6, 10, 14-trimethyl-
1998	103. "CNC99"	Nonylbenzene
1999	104. "CNC100"	Pinonaldehyde
2000	105. "CNC101"	Phthalic acid
2001	106. "CNC102"	4-methyl-Phthalic acid
2002	107. "CNC103"	1,8- Naphthalic acid
2003	108. "CNC104"	2H-1-Benzopyran-2-one